Hydrochemical characteristics and seasonal influence on the pollution by acid mine drainage in the Odiel River Basin (SW Spain).

Aguasanta M. Sarmiento [a]*, José Miguel Nieto [a], Manuel Olías [b], Carlos R. Cánovas [b]

[a] Department of Geology. Faculty of Experimental Sciences. University of Huelva. Avda. Fuerzas Armadas, s/n. 21071-Huelva, Spain.

[b] Department of Geodynamics and Palaeontology. Faculty of Experimental Sciences. University of Huelva. Avda. Fuerzas Armadas, s/n. 21071-Huelva, Spain.

* Corresponding author:

Departamento de Geología, F. Ciencias Experimentales. Campus El Carmen. Universidad de Huelva. Avda. Fuerzas Armadas, s/n. 21071-Huelva, Spain.

Tel: +34 959 219 826; fax: +34 959 219 810

E-mail address: aguasanta.miguel@dgeo.uhu.es (A.M. Sarmiento).

Abstract

The Odiel River Basin is heavily affected by acid mine drainage (AMD) from the sulphide mining areas in the Iberian Pyrite Belt (IPB). We have conducted a thorough study along this fluvial system, monitoring the seasonal influence on the pollution level and its hydrochemical characteristics. From 2002 to 2006, surface water samples were collected in 91 different points throughout the Odiel River Basin and analyzed by field and laboratory methods for dissolved metals and metalloids. Acid mine drainage affects

37% of the length of the drainage network, which shows a great diversity of geochemical conditions as well as significant variations through the hydrological year. Unaffected streams show different water types depending on the lithological substrate and the marine aerosol influence. Mean concentrations in the contaminated streams are very high: 231 mg/L of Fe, 135 mg/L of Al, 56 mg/L of Zn, 16 mg/L of Cu, etc. Four types of contaminated streams were recognized based on hydrochemical and physicochemical characteristics. There are important seasonal variations depending on the precipitation regimen, level of pollution and proximity to the AMD sources. In the more contaminated samples the M/Fe ratio (M = metals other than Fe) decreases during the summer season. Slightly contaminated samples show the inverse evolution as this ratio increases in spring and summer due to substantial Fe precipitation. A recomparison of contaminant loads suggests that the Odiel River Basin (including the Tinto River) accounts for 15% of the global gross flux of dissolved Zn and 3% of the global gross flux of dissolved Cu transported by rivers into the ocean.

Key words: Odiel River, acid mine drainage, seasonal variations, Fe/Metal ratio.

1. Introduction

Acidic drainage is one of the biggest environmental problems caused by mining sulphide-rich mineral deposits. Mining waste can continue to adversely affect the environment for centuries after the abandonment of the mine itself, contaminating the soil in the immediate vicinity and also being dispersed by both surface and ground waters. Although precise quantification of the scale of this pollution is difficult, Johnson and Hallberg (2005) estimated that, in 1989, approximately 19300 km of rivers and

72000 ha of lakes and reservoirs throughout the world were severely affected by mining effluents. Mine drainage results from the oxidation of pyrite and other sulphide minerals generally associated with coal and metal-bearing mineral deposits. Mine drainage is most often acidic and contains high concentrations of metals and metalloids.

In Andalusia (south-western Spain) thousands of years of mining in the Iberian Pyrite Belt (IPB) (Davis et al., 2000; Leblanc et al., 2000; Nocete et al., 2005) has resulted in enormous metal wastes that seriously degrade the environment. Oxidation of the sulphide-rich waste by oxygenated water generates acid mine drainage (AMD), most of which is released into the upper part of the Odiel River Basin, the most important river in Huelva Province. This river (together with the Tinto River) discharges into the Gulf of Cadiz. The pollution load has motivated a large number of studies to assess the processes that control the metal fate and fluxes during estuarine mixing (Elbaz-Poulichet and Dupuy, 1999; Grande et al., 1999; Borrego et al., 2002; Sainz et al., 2004; Nieto et al., 2007). Olías et al (2006) estimated that the Odiel River alone transports enormous amounts of dissolved contaminants: 2847 t/y of Fe, 4557 t/y of Al, 2612 t/y of Zn, 1252 t/y of Cu, 1452 t/y of Mn and minor quantities of other metals (62 t/y of Co, 12 t/y of Pb, etc). Despite natural removal processes (Elbaz-Poulichet et al., 2001a, Braungardt et al., 2003) a significant amount of metals escapes from the estuary and is transferred to the Gulf of Cadiz and to the Mediterranean Sea (Van Geen et al., 1997; Elbaz-Poulichet et al., 2001b).

As productivity in Huelva province changed from mining to agriculture, the contamination of inland water resources in the Odiel River Basin has become a greater concern. However, comparatively few studies have addressed this aspect of the

problem. Sainz et al. (2002) have characterized the chemical composition of the different AMD sources (mine dumps, active mines and abandoned mines) in the Odiel River Basin. Sánchez-España et al. (2005) have studied the physical properties and the water chemistry of leaches from 25 different mines draining off into the upper part of the Odiel River Basin, some of them belonging to the neighbouring Tinto River. Other works have focused on the hydrochemical characteristics of the lower part of the Odiel River before its mouth into the estuary (Olías et al., 2004; Cánovas et al., 2007).

In spite of numerous publications about pollution in the Odiel River, a thorough study connecting the whole basin is necessary from the upper to the lower part of the basin, including tributary streams and leachate from major polluted sources. For this reason, a large research project was started in 2002 sponsored by and in collaboration with several national and regional organisations. Several samplings have been performed since then, so a study of seasonal variation was also possible. The main objectives of this paper are to characterize the water chemistry and the seasonal influence on the pollution level throughout the basin.

2. Site description

2.1. Geology

Most of the Odiel River drainage flows across the IPB (Fig. 1). The IPB extends east to west from Seville Province, across Huelva Province, into Portugal. It is considered to be the biggest sulphide deposit in the world with a length of over 200 km, a width of about 40 km and estimated reserves in the order of 1700 Mt of sulphide ore (Saez et al.,

1999). The IBP belongs to the South Portuguese Zone of the Hercynian Iberian Massif and is formed by upper Palaeozoic materials that can be divided into three lithological groups: 1) the Phyllite-Quartzite Group (PQ), formed by a thick sequence of shales and sandstones, 2) the Volcano-Sedimentary Complex (VSC), including a mafic–felsic volcanic sequence interstratified with shales, and 3) the Culm Group where shales, sandstones and conglomerates prevail. The southern part of the Odiel River flows across Neogene marly sediments from the Guadalquivir depression. In the northern part of the basin plutonic and metamorphic rocks from the Ossa-Morena Zone also outcrop.

Associated with the VSC are many massive polymetallic sulphide deposits (>80). Pyrite (FeS_2) is the main mineral in these deposits, together with lower quantities of sphalerite (ZnS), galena (PbS), chalcopyrite ($CuFeS_2$), arsenopyrite (FeAsS) and other sulphides that contain minor quantities of Cd, Sn, Ag, Au, Co, Hg, etc. Fig. 1 shows the 28 main mines, including Riotinto, Tharsis, Confesionarios and Sotiel, which drain into the Odiel River Basin.

2.2. Hydrology and climatology

The Odiel River Basin is the largest drainage basin in Huelva province, with an area of about 2300 km^2. The Odiel River starts in the Sierra de Aracena and, together with the Tinto River, flows into a coastal wetland known as the Ría of Huelva estuary, which is part of a very important Natural Reserve (Fig. 1).

The Odiel River drops over 600 metres on its way from the headwaters to the mouth, about 140 km away. Its annual flow has been estimated at about 500 hm^3/yr, however

marked variations in this mean occur due to the Mediterranean climate, which includes long periods of drought and intense rainy events. The mean annual rainfall in the basin is 812 mm, 50% of which occurs between October and January. Fig. 2 shows the average rainfall and temperature registered in the basin (Fig. 2a), and the discharge (Fig. 2b) at the stream gauge located before the mouth (see Fig. 1 for location), during the study period.

The Odiel drainage network has a total of 1149 km of streams. The most important tributaries in the basin are the Olivargas, Oraque and Meca on the right bank and the Agrio and Villar on the left bank. Several reservoirs have been built in the Odiel River Basin. The biggest water reservoirs in the basin are Olivargas and Sancho, with a capacity of 29 and 58 hm^3, respectively (Fig. 1).

3. Methodology

3.1. Sampling

Several samplings were performed throughout the whole basin between 2002 and 2006 (Fig. 2b). A total of 478 water samples were collected at points shown in Fig. 1 and listed in Table 1. Of these 91 points, 24 are natural streams unaffected by AMD and the rest (67 points) are streams affected by acidic leachates from 28 different mines. Daily water flow data during the studied period (Fig. 2b) were obtained from a stream-gauging station placed in the southern part of the basin (sampling point 91, Fig. 1). Rainfall (Fig. 2a) was obtained from 23 rain-gauge stations.

Water samples were filtered immediately in field through 0.22 μm Millipore filters fitted on Sartorius polycarbonate filter holders. Samples for cations and metal analysis were acidified in the field to pH<2 with suprapur HNO_3 (2%) and then stored in the dark at 4ºC in polyethylene bottles until analysis. Samples collected for alkalinity and anion determinations were filtered but not acidified. Samples for Fe(II) determination were filtered through 0.1 μm, and the Fe(II) was complexed by adding 0.5 % (w/w) 1,10-phenanthroline chloride solution after buffering to pH=4.5 with an ammonium acetate/acetic buffer (Rodier et al., 1996).

3.2. Analytical determinations

Several physicochemical parameters were measured in the field. Temperature, pH and specific conductance were measured using a portable MX 300 meter (Mettler Toledo). Dissolved oxygen was analysed using a Hanna meter, and redox potential was determined using a Hanna meter with Pt and Ag/AgCl electrode (Crison). The pH meter was calibrated using Hanna standard solutions (pH 4.01 and pH 7.01) and redox potential was checked using Hanna standard solutions (240 mV and 470 mV).

Anions were determined by Ion Chromatography using a Dionex DX-120 fitted with an AS 9-HC of 4 x 250-mm column and a 4-mm ASRS-ULTRA suppressing membrane. Detection limits were 0.1 mg/L for fluoride, nitrate and chloride, and 0.5 mg/L for sulphate. Alkalinity was determined by the titration method (Standard Methods 2320 for the Examination of Water and Wastewater) with standardized HCl and bromcresol green indicator.

Concentrations of dissolved Al, As, Ca, Cd, Co, Cr, Cu, Fe, K, Mg, Mn, Na, Ni, Pb, Sb, Se, Si, Sn, and Zn were determined by Inductively Coupled Plasma Atomic Emission Spectrometry (ICP-AES Jobin-Ybon Ultima2) using a protocol especially designed for AMD samples (Tyler et al., 2004). Analysis was performed at the Central Research Services of the University of Huelva. Multielement standard solutions prepared from single certified standards supplied by SCP SCIENCE were used for calibration. They were run at the beginning and at the end of each analytical series. Certified Reference Material SRM-1640 NIST fresh-water-type and inter-laboratory standard IRMM-N3 wastewater test material, European Commission Institute for Reference Materials and Measurements, were also analysed. Detection limits were calculated by average, and standard deviations from ten blanks. Detection limits were: 200 µg/L for Al, Fe, Mn, Mg, Na, K, Si; 500 µg/L for Ca; 50 µg/L for Zn; 5 µg/L for Cu; 2 µg/L for As and 1 µg/L for the other trace elements.

Fe(II) was determined using colorimetry at 510 nm with a SHIMADZU UVmini-1240 spectrophotometer. The detection limit was 0.3 mg/L and the precision better than 5 %.

3.3. Geochemical modelling

Water chemistry was interpreted with the assistance of the equilibrium chemical-speciation/mass-transfer model PHREEQC (Parkhurst and Appelo, 1999) using the thermodynamic database WATEQ4F (Ball and Nordstrom, 1991). The degree of saturation is expressed as the saturation index (SI), where SI is equal to the difference of logarithms of ion activity product and solubility constant (SI = logIAP - logKsp). WATEQ4F was used to calculate the saturation indices for discrete minerals that may

be controlling the concentrations of dissolved species in the waters. Published solubility constants were used for other minerals, such as schwertmannite.

4. Results and discussion

In the following sections the main results obtained in this work will be discussed. Representative and selected water sample analyses are shown in Tables 6 and 8. The whole dataset available for this work has been published elsewhere (Sarmiento, 2008).

4.1. Hydrochemical characteristics of the uncontaminated stream waters

Table 2 shows the statistical values of 24 uncontaminated streams that provide a chemical reference for background water quality in the area. These streams are characterized by near-neutral pH values (mean 7.2,) and specific conductance that does not exceed 553 µS/cm. Major anions have concentrations between 8.7-75.9 mg/L of SO_4^{2-}, 91-212 mg/L of HCO_3^- and 23-78 mg/L of Cl^-. Uncontaminated waters are characterized by low redox potential (330-480 mV) and average concentrations of Al, Fe, Cu, Mn and Zn <200 µg/L.

Three subgroups can be differentiated by the Piper diagram shown in Fig. 3a. The first group is made up of streams located in the northern part of the studied area (circles in Fig. 3a). Maximum concentrations of bicarbonates and carbonates are found in this group of streams, which drain across the Ossa-Morena Zone (Fig. 1), where limestones crop out. These waters all have pH values >7.5. The second group consists of samples located in the middle and lower part of the area, within the IPB (Fig. 1) where

polymetallic sulphide ores are present, and are characterized by magnesium-sulphate water type (squares in Fig. 3a). The pH values of this group are all <7.5. The last group consists of streams located in the south-western part of the area, and these are sodium-chloride waters (triangles in Fig. 3a) due to the influence of marine aerosols, as will be discussed later.

4.1.1. Seasonal variation

Fig. 3b shows the Piper diagram for the uncontaminated streams sampled in two different seasons: autumn (October 2002, 2004, 2005 and November 2003) and spring (May 2002, 2003, 2004, 2005 and March 2004). Relative bicarbonate concentration as well as pH values are slightly higher in spring, while relative sulphate and chloride concentration decreases. In autumn, the composition is more magnesium-sulphate-rich, and the highest concentration of metals such as Fe (910 μg/L), Al (890 μg/L), Cu (200 μg/L), Pb (24 μg/L), As (7.9 μg/L), etc. are found at this time. This increase in metal concentration can be due to the natural weathering of sulphide minerals thatcrop out in the IPB; the weathering products are washed with the first autumn rains.

4.1.2. Marine aerosol influence on the natural streams

Streams from the south-western part of the basin show a higher average concentration of chloride (78 mg/L) than the overall average (23 mg/L). The absence of evaporite materials in the zone indicates an influence of marine aerosols, as observed by Lorrai and Fanfani (2007). Table 3 shows the correlation matrix between major ions calculated using Spearman coefficients (bold values indicate $p<0.05$). The highest correlations are

found for Na^+, Mg^{2+} and Cl^- (>0.8), which are some of the main components in seawater. Besides, the Cl^-/Na^+ ratio (1.65) of uncontaminated water (discontinuous line in Fig. 4a) is similar to the ratio of seawater (1.8), and the (Na^+, Mg^{2+} and Cl^-) concentration exhibits a general decrease with distance northward (Y-UTM) of the sampling points (Fig. 4b). The three samples collected in reservoirs show a lower concentration possibly because they have trapped more water during spring when the aerosol influence is diminished.

In fact, Fig. 4a also shows the relation between Cl and Na for some samples collected on a single day in autumn (November 9, 2004) and a single day in spring (March 29, 2004). In spring the Cl^-/Na^+ ratio (1.45) is further from the seawater ratio than in autumn. These findings are in accordance with the atmospheric parameters measured: averages of 15.6 and 0.4 mm of rainfall and wind direction of N184º and N312º for the sampling days of autumn and spring, respectively. In the autumn sampling, the wind direction favors aerosol intrusion within the basin and the heavy rainfall on this day contributes to aerosol deposition.

4.2. The contaminated stream waters

4.2.1. Main water courses, assessment of the length of affected streams and contaminant load transported by the Odiel River

Fig. 5 shows the average concentrations of various contaminants along the main course of the major streams in the Odiel River Basin (Odiel and Oraque Rivers), as well as the places where the discharge of mine leachates takes place. The Odiel River starts with a

water quality typical of natural streams. The pH is around 8 and the sulphate concentration is <22 mg/L, but the bicarbonate concentration is about 200 mg/L (near the maximum value in Table 2). Points 1 and 2 represent the background water quality of the river. After receiving the outflows from the first mines (21 km downstream, Fig. 5a), the pH of the Odiel River decreases from 8 to about 5.5, and the contaminant content increases (2 mg/L of Al, 3 mg/L of Fe, 138 mg/L of sulphate, etc). The water quality of the river partially recovers 2 km downstream (point 11: pH of 7, 1 mg/L of Al, 89 mg/L of sulphate, etc.) due to the continued presence of bicarbonate in the water (88 mg/L). After joining Agrio creek that drains part of the Riotinto mining area, the water of the Odiel River is severely spoiled (26 km downstream, Fig. 5a). At this point, the water has an average pH of 3.4 and contains 2409 mg/L of sulphate, 64 mg/L of Fe, 170 mg/L of Al, 18 mg/L of Cu, 38 mg/L of Zn and minor quantities of other toxic elements. Below this point, the contamination levels decrease slightly; however an increase of As (average of 43 µg/L) is observed at the point 43 after joining with Villar Creek, which carries the acid leach from Tinto Santa Rosa mine. In this mine, arsenopyrites were dug out as secondary minerals (Pinedo Vara, 1963). After the point of junction with the leach from Sotiel mine (point 45, fig. 5a), the level of contamination increases again, exhibiting the maximum average concentration of Pb (110 µg/L) along the river. Finally, another important stream is the Meca River (Fig. 1), which is strongly contaminated by the Tharsis mining district and La Lapilla mine.

The last point analysed is located just before the Huelva estuary (Figs. 1, 5a). At this point, the average pH is about 3.5, specific conductance is 1.2 mS/cm, and the water contains 700 mg/L of sulphate, 40 mg/L of Al, 8 mg/L of Mn, 12 mg/L of Zn, 5 mg/L of Cu, 4 mg/L of Fe, 260 µg/L of Co, 85 µg/L of Pb.

Another important stream in the Odiel River Basin is the Oraque River (fig. 5b), which is contaminated at its source mainly by the outflows of the San Telmo mine, and to a lesser degree, by the El Carpio mine, among others. The level of contamination generally decreases downstream. However, the concentration of Pb slightly increases up to 45 μg/L, due to the discharges from La Joya, Lomero Poyatos and Confesionarios mines. These mines have galena and other Pb-containing secondary minerals (Pinedo Vara, 1963). The pollution increases before the point of junction with the Odiel River again, due to the high contaminant load from the Tharsis mine.

From a total of 1149 km of the river network examined, 427 km are affected by AMD (37% of the total). Analysing the results by sub-basins, we observed that the sub-basins with the longest courses of contaminated water are those of the Odiel, with 222 km (36%) and the Oraque, with 141 km (39%), followed by the Meca basin (36%). These results are higher than those obtained by Sánchez-España et al. (2005).

Contamination load transported by the Odiel and Tinto rivers into the Huelva estuary and the Atlantic Ocean was estimated by Olías et al., 2006. The analytical data used for that study were results of sampling programs covering several years. In the Odiel river the sample station was located at the point 91 (Fig. 1). The values obtained were compared with the estimations published by GESAMP (1987) of the global gross flux of dissolved metals transported by rivers into the oceans. In the present work, a recomparison with the global gross flux has been estimated based on the compilation made by Gaillardet et al (2003) for the mean values of trace elements input to the estuaries and ocean by selecting the largest rivers of the World (Table 4). The global

gross flux of sulphate has been based on the result obtained by Meybeck (2003) for the estimation of anthropogenic sulphate input to ocean (Table 4).These new percentages are substantially lower than those obtained by Olías et al (2006), however the values are still surprising. The load transported by both rivers represents 3% of the global gross flux of Cu and 15% of the Zn, coming mainly from the Odiel load (Table 4).

4.2.2. Hydrochemical characteristics

The mean chemical composition and range of the contaminated streams in the Odiel River Basin are listed in Table 5. The results are characterized by large variations in pH (2 – 8.6), specific conductance (0.2 – 18.5 mS/cm), dissolved oxygen (1.5 – 13.4 mg/L) and redox potential (211 – 813 mV), which illustrates the great diversity of geochemical conditions in the drainage systems. Contaminated samples show an excellent correlation (R^2=0.73; ρ<0.05) between pH and redox potential. Most of the samples are high in sulphate concentration with values between 500 and 36000 mg/L, dependent on pH values. Sulphate concentration also shows a high correlation (R^2=0.99; ρ<0.05) with the specific conductance, and to most of the measured metal and metalloids like Al, Fe, Cu, Co, Zn, etc.

Most elements show large variations in concentration; for example, Fe (0.2 - 4280 mg/L), Zn (0.2 - 860 mg/L), Cu (0.2 – 16 mg/L). Maximum concentrations of many "trace" metals are high; for example, As (up to 7.4 mg/L), Co (up to 31 mg/L), Ni (up to 14 mg/L), Pb (up to 6 mg/L). The high acidity generated during the oxidizing process gives rise to accelerated hydrolysis of other minerals in the spoil materials, mobilizing large quantities of their constituent elements, such as Al (up to 2000 mg/L), Ca (up to

1100 mg/L), Mg (2900 mg/L), Mn (374 mg/L), etc. The maximum concentrations are connected with the minimum pH, so an excellent relationship between specific conductance and pH has been found ($r = -0.88$; $\rho<0.05$, $n = 425$).

As Nordstrom (2000) showed, the waters which have sufficient iron concentration give an equilibrium potential at the platinum electrode for the Fe(II)/(III) redox couple. The relationship between Eh measured in the field with theoretical Eh values calculated from Fe(II)/(III) determinations in the affected Odiel-waters is high ($R^2 = 0.94$, $n = 90$). The comparison of measured and calculated Eh shows a strong correlation for samples with total iron concentration greater than 10^{-5} molal.

4.2.3. Types of stream waters affected by acid mine drainage

Fig. 6 shows the relationships between redox potential and pH, specific conductance, dissolved oxygen and Fe^{2+}/Fe_t ratio for the contaminated samples. The distribution of the Fe species may be described by a Boltzmann model (Fig. 6d), so the redox potential for $(Fe^{2+}/Fe^{3+}) = 1$ can be calculated (Eh = 715 mV). This Eh value is slightly different than the one used by Sánchez-España et al. (2005) (640 mV).In relation to the composition and physicochemical parameters, four groups of streams can be differentiated based on their origin, the level of influence of oxidation of sulphides and the extent of neutralisation of the acidity generated.. A representative selection of samples belonging to these groups is listed in Table 6.

Type I: samples showing redox potential between 650 – 750 mV (Fig. 6d) and dissolved oxygen saturation below 60% (Fig. 6c). These streams are strongly affected by

oxidation of sulphides and are at or near the AMD sources, essentially acidic leachates which have not undergone dilution or precipitation processes. They are extremely acid (pH<3, Fig. 6a), specific conductance is >4 mS/cm (Fig. 6b) and Fe^{2+}/Fe_t ratio higher than 0.7 (Fig. 6d). They all show similar characteristics in connection with the elements associated to the oxidation of sulphides, carrying high quantities of metals and sulphates, including the highest concentrations of Fe (4300 mg/L), Cu (321 mg/L), Zn (860 mg/L), Ni (14.4 mg/L), Co (31 mg/L), As (7.5 mg/L) and Cd (2.2 mg/L). The molar ratio of Fe/SO_4^{2-} theoretically obtained from the oxidation of pyrite is 0.5 (Fig. 7). This group of waters has Fe/SO_4^{2-} ratios close to this value (Fig. 7b: red squares, R^2 = 0.98; Fe/SO_4^{2-} = 0.497).

Type II: samples showing redox potential higher than 750 mV. This group of streams is strongly affected by AMD but is not so close to the mining sites. They are strongly oxic and acidic waters (pH<3, Fig. 6a) with saturation of dissolved oxygen higher than 80% (Fig. 6c). Fe(II) is oxidized to Fe(III) due to bacterial activity and aeration processes when leachates flow along surface streams, so the ratio Fe(II)/Fe decreases (less than 0.3, Fig. 6d). The specific conductance is <5 mS/cm (Fig. 6b) due in part to precipitation of Fe(III)-containing species.

Type III: samples showing redox potential between 650 – 750 mV and dissolved oxygen saturation higher than 60% (Fig. 6c). These streams are strongly affected by AMD but have undergone neutralisation processes. Carbonate minerals are practically non-existent in the IPB, so the neutralization is basically due to dilution by uncontaminated water (Cánovas et al., 2007) and to hydrolysis of aluminosilicate minerals. In these samples pH increases (up to 4, Fig. 6a), and specific conductance

decreases (generally less than 4 mS/cm, Fig. 6b). Fe concentration is moderately low (less than 100 mg/L) and Fe^{2+}/Fe ratio shows large variations according to the dissolved oxygen saturation (Fig. 6d). The most relevant characteristic of these streams are the high concentrations of Ca, Al, Mg and Mn and relatively low Fe contents, which indicates that significant processes involving the precipitation of Fe compounds occurred.

Type IV: waters showing redox potential less than 650 mV. These streams are slightly affected by AMD or strongly neutralised. Iron concentration is very low and only present as Fe(II). The pH values are close to neutrality and specific conductance and toxic element concentrations are low.

Fig. 8 shows the four different types of samples according to the Ficklin diagram (Plumlee et al., 1992) for the composition of mine drainages. The Ficklin diagram classifies waters based on their pH and the sum of base metals Zn, Cu, Pb, Cd, Co and Ni. The four types of samples can be explained as the result of natural attenuation of acidic leachates (Lambeth, 1999). The evolution would be that indicated by the arrow in Fig. 8. Leachates originating from sulphide oxidation have low values of pH and dissolved oxygen, carrying in solution high quantities of Fe(II) and toxic elements (Type I). When water contacts atmospheric oxygen, Fe(II) is oxidized to Fe(III), involving Fe(III) precipitation, so redox potential increases, whereas pH remains constant and metal concentration decreases (Type II). When these leaches are mixed with uncontaminated waters or neutralised by dissolution of aluminosilicates, the pH increases and the dissolved Fe(III) precipitates (Type III). If the dilution processes are strong and pH is near neutrality, most of the Fe and toxic metals precipitate (Type IV).

The evolution along a stream (Meca River) is shown in the Fig. 8 as black star symbols (see Fig. 1 for location). Sample number 80 belongs to the leach originated in the La Lapilla mine; the Fe concentration is around 4300 mg/L and the pH is 2.4 (type I). A few kilometres downstream the water composition barely undergoes dilution; however sample 81 shows a pH of 2.6 and the Fe concentration decreases to 220 mg/L. The concentration of the rest of the elements also decreases (type II). At point 88 (Fig. 1), the Meca River receives waters from others streams and the pH increases to 3.4 and the Fe concentration decreases to 20 mg/L (type III). Finally, the stream flows into a reservoir (sample 90) where a large dilution process occurs. In this point, the pH of the water increases to 4.7 and the Fe concentration is below detection limit (type IV). The Odiel river has a high discharge of good quality water in its headwaters, so the polluted samples from the main course of the Odiel River only belong to types III and IV due to dilution processes.

4.2.4. Seasonal variation

Hydrochemical characteristics in the Odiel River Basin undergo significant seasonal changes due to climatological variations, and our frequent samplings during the hydrologic year (2003/2004) provide the data needed to study this process. Table 7 shows the average values of parameters measured in some samplings performed during the hydrologic year 2003/2004. The number of samples decreases in the dry season (June and August) due to the absence of water in many of the streams. Some gaps exist in the discharge record at point 91, but the time lag between rainfall and discharge response is low (Fig. 2). As a result, the accumulated rainfall (measured at 23 rain

gauges) for the 30-day period prior to each sampling has been used in evaluating the seasonal variation of the contamination.

Fig. 9 displays the relationship between rainfall and the average values of pH and specific conductance. As expected, pH values are slightly higher as rainfall increases. So the average pH is maximum in February (4.3) and minimum in August (3.0), when the waters come mainly from the mining leaches without dilution processes. In general, the composition of the samples follows an evolution similar to the specific conductance.

While sulphate, metal and metalloid contents decrease due to dilution processes owing to rainfall, the temporal evolution is significantly different depending on the stream pollution level. Fig. 10 displays the Principal Component Analysis on the measured parameters for two different types of streams. The slightly affected streams do not undergo great changes in their chemical composition, although there are clear differences between wet season (November, January, February, March and May) and dry season (June and August). On the contrary, the highly polluted streams are strongly influenced by rainfall events, showing a great variation depending on previous rainfall.

Although in both cases the level of contamination increases as rainfall decreases, M/Fe ratio does not undergo the same evolution (M represents elements such as Al, Cu, Zn and Mn). Fig. 11 shows a schematic plot of M/Fe ratios versus pH and the difference in seasonal affects in relation to the pollution level. Fig. 12 shows the Fe/SO_4^{2-} ratio for two slightly polluted samples (points 91 and 34) and two highly polluted samples (points 65 and 15; see Fig. 1 for location). M/Fe ratio increases from wet to dry season in the slightly affected samples, while it decreases in the strongly affected samples. In

the dry and warm season, close to the pollution sources, sulphide oxidation processes increase. In the absence of dilution, the pH decreases to the point where Fe precipitation drops off. As a result, the M/Fe ratio decreases, and the Fe/SO_4^{2-} ratio increases (Figs. 11, 12) in the strongly affected streams. In the slightly affected streams, the pH drop in the dry season is insufficient to prevent Fe precipitation, which occurs due to evaporation processes. Hence the M/Fe ratio increases while the Fe/SO_4^{2-} ratio decreases in these streams during the dry season. Thus in summer, Fe mobility is lower in the slightly affected streams than in the more affected streams. These results demonstrate the importance of collecting seasonal data in the study of contaminant transport in this system.

As mentioned above, the main contaminant sources are located in the upper part of the basin, so the seasonal effect on the contamination should be different depending on the basin sector. Fig. 13a shows the evolution of Al concentration during the studied period in three sectors of the Odiel River (see Fig. 1 for location). The concentration strongly increases during the dry season and decreases in the wet season at the upper and middle parts of the basin. At the lower part, the variation in the concentration is less pronounced, remaining practically constant all year long (except in the February sample collected after a large rainfall). However, in October 2004 coinciding with the first autumn rains, an increase in the concentration was observed only in the lower part. This last finding is explained by the rinse out of soluble efflorescent sulphate salts precipitated during the dry season along the river margins (Olías et al., 2004, Cánovas et al., 2007). Most of elements show a similar evolution. Table 8 shows the analytical data for the three sampling points along the studied period (shadowed data belong to the same hydrological year).

The Fe concentration undergoes a similar evolution in the upper and middle basin, though the variation in the upper basin is larger than for Al and the other elements (Fig. 13b). In contrast, Fe concentration decreases strongly in the first months of the dry season in the lowest part of the basin, in accordance with the aforementioned mobility of Fe.

4.2.5. Seasonal variation on the mineral saturation indexes

Major Fe oxyhydroxy-sulphates in acid mine waters are: K-jarosite ($KFe_3(SO_4)_2(OH)_6$), ferrihydrite ($Fe(OH)_3$) and schwertmannite ($Fe_8O_8(OH)_6(SO_4)$). Jarosite is found in very acid environments, schwertmannite predominates over pH values between 3 and 4, and ferrihydrite and goethite are formed at pH values from 5 to 7 (Murad and Rojik, 2003).

Saturation index values have been calculated for the contaminated samples using thermodynamic constants from the geochemical database WATEQ4F for jarosite, ferrihydrite and goethite equilibrium. Constants from Yu et al. (1999) have been used for schwertmannite. Most of the samples are supersaturated in schwertmannite, the higher saturation indexes are observed at high pH and low Eh values. Generally samples supersaturated in K-jarosite show Eh >600 mV and pH less than 4. On the other hand, most of the samples supersaturated in ferrihydrite have Eh <600 mV, low specific conductance and high pH and dissolved oxygen. Goethite is supersaturated in all the samples, however it does not usually appear as a direct precipitate due to its slow precipitation kinetics, but it is formed by transformation from the above mentioned Fe oxyhydroxide sulphates (Bigham et al., 1996; Nordstrom and Alpers 1999; Acero et al.,

2006). In relation to the different types of contaminated samples in Fig. 6, samples in all groups will be saturated in schwertmannite. Types I and II are generally saturated in K-jarosite while types III and IV are saturated in ferrihydrite.The large degrees of supersaturation for ferrihydrite, jarosite, and schwertmannite found in these waters could be related to the iron nanocolloids that pass through the filtration (Bigham and Nordstrom, 2000), considering "nanocolloids" as colloids that passes through a 0.1 μm membrane filter.

Fig. 14 shows the evolution of the saturation index values during the hydrological year at three different sites on the Odiel River. In the wet season, the saturation indexes of schwertmannite and ferrihydrite are higher in the lowest part of the river, while in the dry season they are higher in the upper part. During the autumn rainfalls (November and January), the only zone supersaturated in K-jarosite is the lowest part, whereas after February it is the highest part. The upper part of the Odiel River is supersaturated all year with respect to schwertmannite. It is supersaturated with respect to jarosite during the dry season and in ferrihydrite only during periods of strong rainfall (like February). The lower part of the basin is supersaturated with respect to schwertmannite and jarosite during the first months of rain. The rinse-out effect in October of 2004, discussed previously, shows up as an increase of the saturation indexes for schwertmannite and jarosite in the lower part of the river, while in the upper part they begin to decrease.

Minerals which could control Al solubility in acidic waters are jurbanite ($Al(SO_4)(OH)\cdot 5H_2O$, alunite ($KAl_3(SO_4)_2(OH)_6$), basaluminite ($Al_4(SO_4)(OH)_{10}\cdot 5H_2O$), gibssite and amorphous $Al(OH)_3$ (Nordstrom, 1982). Previous works point out that, despite its apparent thermodynamic stability, jurbanite is not important as Al solubility

control in AMD (Nordstrom and Alpers, 1999; Bigham and Nordstrom, 2000; Blowes et al., 2004). Sánchez-España et al (2005) suggest that basaluminite is the mineral that best explains the Al behaviour of acidic solutions at pH below 5 in the IPB. On the other hand, Cánovas et al (2007) indicate that alunite is the most stable phase at a point in the lower part of the Odiel River Basin.

Thermodynamic constants from the WATEQ4F database for alunite, basaluminite and amorphous $Al(OH)_3$ have also been calculated during the hydrological year (Fig. 14). Amorphous $Al(OH)_3$ is undersaturated throughout the year, having higher saturation indexes in the wet season, mainly in the lower part. Basaluminite and alunite follow a similar evolution, although while alunite is supersaturated or near saturation, basaluminite is strongly undersaturated in summer, in agreement with Cánovas et al (2007). However, precipitation of basaluminite could occur in the northern section of the river in the wetter periods, in accordance with the observations by Sánchez-España et al. (2005).

5. Conclusions

In consequence of the intense mining activity in the province of Huelva, the streams in the Odiel River Basin show a high degree of pollution. Polluted streams sampled in this study have mean pH values of 3.6, 2700 mg/L of sulphates 231 mg/L of Fe, 135 mg/L of Al, 56 mg/L of Zn, 28 mg/L of Mn and 16 mg/L of Cu. Of the total 1149 km in the examined river network, 427 km are affected by AMD, meaning 37% of the total basin. The load transported by Odiel River into the Huelva estuary and Atlantic Ocean represents almost 3% of the global gross flux of Cu and 15% of the Zn.

In the Odiel River Basin, four groups of contaminated streams can be differentiated based on the level of contamination and degree of natural attenuation. Type I: Strongly affected streams that are at or near the AMD sources and are acidic leachates which have not undergone dilution or precipitation processes. Type II: Strongly affected streams that are acidic leachates which have undergone precipitation processes. Type III: Affected streams slightly neutralised by uncontaminated waters or dissolution of aluminosilicates. Type IV: Slightly affected or strongly neutralised streams.

Hydrochemical and mineralogical AMD-processes in the Odiel River Basin show different patterns depending on factors such as seasonal variations, contamination levels and location in the basin. These processes also affect the uncontaminated streams, so that in autumn coinciding with the first rains, sulphate and metal concentration increases while pH values and bicarbonate concentration decrease due to the natural weathering of sulphide materials outcropping in the zone. In addition, these uncontaminated streams are influenced by marine aerosols from the Atlantic Ocean.

In the contaminated streams, while sulphate, metal and metalloid contents decrease due to dilution processes owing to rainfall, the temporal evolution is significantly different depending on the stream pollution level. The slightly affected streams do not undergo great changes in their chemical composition, although there are clear differences between wet season and dry season. On the contrary, the highly polluted streams are strongly influenced by rainfall events, showing a great variation depending on previous rainfall. Although in both cases the level of contamination increases as rainfall decreases, metal/Fe ratio does not undergo the same evolution. Metal/Fe ratio increases

from wet to dry season in the slightly affected samples, while it decreases in the strongly affected samples.

Most elements show a similar evolution along the Odiel River. In general, the concentrations increase during the dry season and decrease in the wet period, except with the first autumn rains, where an increase in the concentration of some elements is observed in the lowest part of the basin and results from the rinse out of soluble salts. In contrast, Fe concentration decreases strongly in the first months of the dry season in the lowest part of the Odiel River.

The strongly affected samples (types I and II) are generally saturated in K-jarosite while the slightly affected samples (types III and IV) are saturated in ferrihydrite. In the wet season the saturation indexes of schwertmannite and ferrihydrite are higher in the lowest part of the river, while in the dry season they are higher in the upper part. During the first autumn rainfalls, the only zone supersaturated in K-jarosite is the lowest part, whereas after February it is the highest part. Basaluminite and alunite can control Al solubility depending on the seasonal and locational variations. Alunite is always supersaturated or near saturation and basaluminite is subsaturated in summer. However, precipitation of basaluminite can occur in the northern section of the river in the wetter periods.

Acknowledgements

This study has been financed by the Spanish Ministry of Science through project CTM2007-66724-C02-02/TECNO and by the Environmental Council of the Andalusia

Regional Government. The authors wish to express their sincere gratitude to Dr. William C. Evans and Dr. Kirk Nordstrom for their detail and helpful comments and suggestions that helped to significantly improve and clarify the original manuscript.

References

Acero, P., Ayora, C., Torrento, C., Nieto, J. M., 2006. The behavior of trace elements during schwertmannite precipitation and subsequent transformation into goethite and jarosite. Geochim. Cosmochim. Acta. 70, 4130-4139.

Ball, J. W., Nordstrom, D. K., 1991. User's manual for WATEQ4F, with revised thermodynamic data base and test cases for calculating speciation of major, trace, and redox elements in natural waters. U.S. Geol. Surv. Open-File Rep. 91-183.

Bigham, J.M., Schwertmann, U., Traina, S.J., Winland, R.L., Wolf, M., 1996. Schwertmannite and the chemical modelling of iron in acid sulphate waters. Geochim. Cosmochim. Acta. 60, 2111-2121.

Bigham, J.M., Nordstrom, D.K., 2000. Iron and hydroxysulfates from acid sulfate waters. In: Alpers, C.N., Jambor, J.L., Nordstrom, D.K. (Eds.) Sulfate minerals: crystallography, geochemistry and environmental significance. Reviews in mineralogy and geochemistry. Mineralogical Society of America. 40, 351-403.

Blowes, D.W., Ptacek C.J., Jambor, J.L., Weisener, C.G., 2004. The geochemistry of acid mine drainage. In: Treatise on geochemistry. Environmental geochemistry, Vol. 9, Elsevier. Ed. Lollar, B. S., 149-204.

Borrego, J., Morales, J.A., de la Torre, M.L., Grande, J.A., 2002. Geochemical characteristics of heavy metal pollution in surface sediments of the Tinto and Odiel river estuary (southwestern Spain). Environ Geol. 41, 785-796.

Braungardt, C.B., Achterberg, E.P., Elbaz-Poulichet, F., Morley, N.H., 2003. Metal geochemistry in a mine polluted estuarine system in Spain. Appl. Geochem. 18, 1757-1771.

Cánovas, C.R., Olías, M., Nieto, J.M., Sarmiento, A.M., Cerón, J.C., 2007. Hydrogeochemical characteristics of the Tinto and Odiel rivers (SW Spain). Factor controlling metal contents. Sci. Total. Environ. 373, 363-382.

Davis, R.A., Welty, A.T., Borrego, J., Morales, J.A., Pendon, J.G., Ryan, J.G., 2000. Rio Tinto estuary (Spain): 5000 years of pollution. Environ. Geol. 39, 1107-1116.

Elbaz-Poulichet, F., Dupuy, C., 1999. Behavior of rare earth elements at the frexhwater-seawater interface of two acid mine rivers: the Tinto and Odiel (Andalucia, Spain). Appl. Geochem. 14, 1063-1072.

Elbaz-Poulichet, F., Morley, N.H., Beckers, J.M., Nomerange, P., 2001a. Metal fluxes through the Strait of Gibraltar: the influence of the Tinto and Odiel rivers (SW Spain). Mar Chem. 73, 193-213.

Elbaz-Poulichet, F., Braungardt, C., Achterberg, E., Morley, N., Cossa, D., Beckers, J.M., Nomerange, P., Cruzado, A., Leblanc, M., 2001b. Metal biogeochemistry in the Tinto-Odiel rivers (Southern Spain) and in the Gulf of Cadiz: a synthesis of the results of TOROS project. Cont Shelf Res. 21, 1961-1973.

Gaillardet, J., Viers, J., Dupré, B., 2003. Trace elements in river waters. In: Holland, H.D., Turekian, K.K. (Eds). Surface and ground water, weathering, and soils. Vol. 5. Treatise on Geochemistry. Elsevier, Oxford, pp. 225-272

GESAMP, 1987. Land/sea boundary flux of contaminants: contributions from rivers. Reports and Studies No. 32. IM0/FAO/UNESCO/WMO/WHO/IAEA/UN/UNEP Group of Experts on the Scientific Aspects of Marine Pollution. Paris.

Grande, J.A., Borrego, J., Morales, J.A., 1999. A study of heavy metal pollution in the Tinto-Odiel estuary in southwestern Spain using factor analysis. Environ Geol. 39, 1095-1101.

Hudson-Edwards, K.A., Schell, C., Macklin, M.G., 1999. Mineralogy and geochemistry of alluvium contamined by metal mining in the Rio Tinto area, southwest Spain. Appl Geochem. 14, 1015-1030.

Johnson, D.B., Hallberg, K.B., 2005. Acid mine drainage remediation options: a review. Sci Total Environ. 338, 3-14.

Lambeth, R.H., 1999. Natural attenuation of acidic drainage from sulfidic tailings at a site in Washington State. In: Filipek, L.H., Plumlee, G.S. (Eds). The environmental geochemistry of mineral deposits, Part B. Case Studies and Researc Topics: Society of Economic Geologists, Rev. Econ. Geol. 6B, pp. 479-491.

Leblanc, M., Morales, J.A., Borrego, J., Elbaz-Poulichet, F., 2000. 4500-year-old mining pollution in Southwestern Spain: long-term implications for modern mining pollution. Econ Geol. 65, 655-662.

Lorrai, M., Fanfani, L., 2007. Effect of sea spray on the chemistry of granitoid aquifers in coastal areas. In: Bullen, T.D., Wang, Y. (Eds.), Proc. 12th International Symposium on Water-Rock-Interaction. Taylor and Francis, London, pp. 1089-1092.

Meybeck, M., 2003. Global occurrence of major elements in rivers. In: Holland, H.D., Turekian, K.K. (Eds). Surface and ground water, weathering, and soils. Vol. 5. Treatise on Geochemistry. Elsevier, Oxford, pp. 207-223.

Murad, E., Rojik, P., 2003. Iron-rich precipitates in a mine drainage environment: influence of pH on mineralogy. Am Mineral. 88,1915–8.

Nieto, J.M., Sarmiento, A.M., Olías, M., Cánovas, C.R., Riba, I., Kalman, J., Delvalls, T.A., 2007. Acid mine drainage pollution in the Tinto and Odiel Rivers (Iberian Pyrite Belt, SW Spain) and bioavailability of the transported metals to the Huelva estuary. Environ Int. 33, 445-455.

Nocete, F., Saez, R., Nieto, J.M., Cruz-Aunon, R., Cabrero, R., Alex, E., Bayona, M.R., 2005. Circulation of silicified oolitic limestone blades in South-Iberia (Spain and Portugal) during the third millennium B.C.: an expression of a core/periphery framework. J Anthropol Archaeol. 24, 62-81.

Nordstrom, D. K., 1982. The effect of sulfate on aluminum concentrations in natural waters: some stability relations in the system Al_2O_3-SO_3-H_2O at 298 K. Geochim Cosmochim Acta. 46, 681-692.

Nordstrom, D.K., Alpers, C.N., 1999. Geochemistry of acid mine waters. In: Plumlee, G.S., Logsdon, M.J. (Eds.), The Environmental Geochemistry of Mineral Deposits, Part A: Processes, Techniques, and Health Issues: Society of Economic Geologists, Rev econ geol., 6A, pp. 133-160.

Nordstrom D.K., 2000. Advances in the hydrogeochemistry and microbiology of acid mine waters. Int Geol Rev. 42, 499-515.

Olías, M., Nieto, .JM., Sarmiento, A.M., Cerón, J.C., Canovas, C.R., 2004. Seasonal water quality variations in a river affected by acid mine drainage: The Odiel river (south west Spain). Sci Total Environ. 333, 267-281.

Olías, M., Cánovas, C., Nieto, J.M., Sarmiento, A.M., 2006. Evaluation of the dissolved contaminant load transported by the Tinto and Odiel rivers (South West Spain). Appl Geochem. 21, 1733-1749.

Parkhurst, D. L. and Appelo, C. A. J., 1999. User's guide to PHREEQC - A computer program for speciation, reactionpath, 1D-transport, and inverse geochemical calculations. U.S. Geological Survey, Water-Resour. Investig. Rep. 99-4259, Denver-Colorado.

Pinedo Vara I., 1963. Piritas de Huelva. Su historia, minería y aprovechamiento. Madrid, Spain. Ed. Summa.

Plumlee, G.S., Smith, K.S., Ficklin, W.H., Briggs, P.H., 1992. Geological and geochemical controls on the composition of mine drainages and natural drainages in mineralized areas. Proceeding, 7th International Water-Rock Interaction Conference, Park City, Utah, 419-422.

Rodier, J., Broutin, J. P., Chambon, P., Champsaur, H., Rodi, L., 1996. L'analyse de l'eau. Dunod, Paris, 1383 pp.

Sáez, R., Pascual, E., Toscano, M., Almodovar, G.R., 1999. The Iberian type of volcano-sedimentary massive sulphide deposits. Miner Deposita. 34, 549-570.

Sainz, A., Grande, J.A., de la Torre, M.L,. Sanchez-Rodas, D., 2002. Characterisation of sequential leachate discharges of mining waste rock dumps in the Tinto and Odiel rivers. J Environ Manage. 64, 345-353.

Sainz ,A., Grande, J.A., de la Torre, M.L., 2004. Characterisation of heavy metal discharge into the Ria of Huelva. Environ Int. 30, 557-566.

Sánchez España, J., López Pamo, E., Santofimia, E., Reyes, J., Barettino, D., 2005. Acid mine drainage in the Iberian Pyrite Belt (Odiel river watershed, Huelva, SW Spain): Geochemistry, mineralogy and environmental implications. Appl Geochem. 20, 1320-1356.

Sarmiento, A.M., 2008. Study of the pollution by acid mine drainage of the surface waters in the Odiel basin (SW Spain). Ph. D. Thesis, University of Huelva, Spain. UMI ProQuest, Publ. No.: AAT 3282346. Ann Arbor, USA. 352 pp. Available from:<http://proquest.umi.com/pqdweb?did=1404342661&sid=3&Fmt=2&clientId=40400&RQT=309&VName=PQD>.

Tyler, G., Carrasco, R., Nieto, J.M., Perez, R., Ruiz, M.J., Sarmiento, A.M., 2004. Optimization of mayor and trace element determination on Acid Mine Drainage samples by Ultrasonic Nebulizer-ICP-OES (USN-ICP-OES) Pittcon Conference, 7-12 March. Chicago, USA. 9000/1000.

van Geen, A., Adkins, J.F., Boyle, E.A., Nelson, C.H., Palanques, A., 1997. A 120 year record of widespread contamination of the Iberian pyrite belt. Geology. 25, 291-284.

Yu, J. Y., Heo, B., Choi, I. K., Cho, J. P., Chang H. W., 1999. Apparent solubilities of schwertmannite and ferrihydrite in natural stream waters polluted by mine drainage. Geochim Cosmochim Acta. 63, 3407-3416.

Table 1. Geographic location (UTM coordinates, USO 29) of the sampling points and pollution sources of the water streams studied (see Fig. 1 for location).

Nº	X-utm	Y-utm	Water streams	n	Pollution sources
1	187267	4189884	Odiel River	2	Not affected
2	180763	4189116	Odiel Reservoir	2	Not affected
3	177320	4190929	Sta. Eulalia Creek	2	Not affected
4	178040	4187282	Odiel River	2	Not affected
5	177897	4187064	Bco Diques	5	Concepción mine
6	175983	4185571	Bco Esperanza	5	Esperanza mine
7	176906	4184779	Palomino Creek	6	El Soldado mine
8	176914	4184597	Bco de los Bardales	7	Poderosa mine
9	176564	4184543	Odiel River	7	Several mines
10	175850	4184338	Bco. Hocino	2	Not affected
11	174974	4182621	Odiel River	6	Several mines
12	179556	4182403	Bco. Escorial	5	Riotinto mine
13	179118	4180850	Tintillo Creek	8	Riotinto mine
14	174970	4182319	Agrio Creek	11	Riotinto mine
15	173275	4182108	Odiel River	17	Several mines
16	172882	4184764	Seca Creek	8	Angostura mine
17	169416	4186476	Escalada Creek	2	Not affected
18	169395	4186389	Escalada Creek	4	San Miguel mine
19	169369	4186322	Escalada Creek	4	San Miguel mine
20	160470	4189217	Bco. Fuente del Valle	3	Confesionarios mine
21	162167	4188926	Bco. Fuente del Valle	3	Aguasteñidas mine
22	162751	4191749	Bco. de Valdelaniña	2	Not affected
23	162545	4189223	Asturianos Reservoir	2	Not affected
24	166030	4187667	Bco. Monte Romero	2	Monte Romero mine
25	165837	4187962	Bco. Monte Romero	4	Cueva de la Mora mine
26	165639	4187677	Bco. Monte Romero	11	Cueva de la Mora mine
27	165069	4186591	Bco. Monte Romero	3	Cueva de la Mora mine
28	164935	4186637	Bco. del Chorrero	2	Not affected
29	164910	4186504	Bco. de Malena	4	Several mines
30	161628	4188002	Bco. de Herrerito	5	La Zarza mine
31	164175	4181042	Olivargas Reservoir	8	Several mines
32	161465	4178983	Bco. de Majofre	4	Perrunal mine
33	163290	4177241	Olivargas Creek	4	Several mines
34	163309	4173341	Odiel River	14	Several mines
35	171599	4177905	Villar Creek	2	Not affected
36	168825	4174677	Villar Creek	2	Not affected
37	168918	4174373	Bco. Palanco	2	Not affected
38	167820	4173103	Los Coladeros Creek	7	Buitrón mine
39	164421	4171995	Villar Creek	4	Several mines
40	164488	4172184	Bco Santa Rosa	5	Tinto Santa Rosa mine
41	164425	4172116	Villar Creek	3	Several mines
42	162416	4171648	Bco. del Batán	3	Almagreras mine
43	162622	4171216	Odiel River	5	Several mines
44	160300	4168680	Bco de las Cañas	7	Sotiel mine
45	160504	4167970	Odiel River	17	Several mines
46	161890	4162693	Bco. Aguas Agrias	3	Several mines
47	162982	4161086	Agua Agria Creek	4	Cruz Infante mine
48	161120	4160769	Campanario reservoir	2	Not affected
49	158399	4169207	Calabazar reservoir	2	Not affected
50	156082	4168931	Riscoso reservoir	2	Not affected
51	156554	4167711	Galaparosa Creek	2	Not affected
52	156544	4167640	Galaparosa Creek	2	Not affected
53	156694	4167713	Bco. Torerera	5	Torerera mine
54	156522	4167530	Galaparosa Creek	5	Torerera mine
55	154979	4191491	Pelada Creek	2	Not affected
56	154758	4191393	Bco Lomero	5	Lomero mine
57	154775	4191231	Pelada Creek	4	Lomero mine
58	156923	4188603	Bco. Gonzalo	6	Confesionarios mine
59	154673	4190559	Pelada Creek	6	Lomero mine
60	152542	4184504	Pelada Creek	5	Several mines
61	148617	4180689	Pelada Creek	5	Several mines
62	158812	4180469	Bco. de la Rondano	3	Perrunal mine
63	154575	4176853	Bco. del Tamujoso	9	Perrunal mine
64	148963	4192009	Panera Creek	2	El Carpio mine
65	149084	4191901	Bco. de Aguas Agrias	11	San Telmo mine
66	149861	4191130	Bco. de Aguas Agrias	6	San Telmo mine
67	146805	4188821	Panera Creek	6	San Telmo mine
68	151730	4189351	Bco. del Fresno	5	Several mines
69	147421	4181457	Fresnera Creek	9	Several mines
70	142774	4180300	Bco. Sepultura	2	Not affected
71	147351	4172802	Oraque River	9	Several mines
72	145777	4172736	Chapinero Creek	2	Not affected
73	145117	4171565	Monte La Osa Creek	2	Not affected
74	148502	4170252	Oraque River	7	Several mines
75	137651	4170713	Grande Reservoir	5	Tharsis mines
76	140667	4169404	Agua Agria Creek	16	Tharsis mines
77	147728	4161536	Oraque River	13	Several mines
78	136036	4165941	Bco. del Val de Oscuro	8	Tharsis mines
79	138046	4163765	Bco. del Oro	7	Tharsis mines
80	138889	4167141	Agustanos Creek	4	La Lapilla mine
81	139436	4163566	Agustanos Creek	6	Several mines
82	133892	4168727	Saucito Creek	5	Tharsis mines
83	132932	4165300	Dehesa Boyal Creek	5	Tharsis mines
84	133641	4165153	Bco. Cebollar	2	Not affected
85	133024	4163126	Dehesa Boyal Creek	5	Tharsis mines
86	134815	4161711	Dehesa Boyal Creek	7	Tharsis mines
87	134908	4159210	Aserrador Creek	2	Not affected
88	139524	4156992	Meca River	6	Several mines
89	135146	4155521	De las Multas Creek	2	Not affected
90	147858	4153695	Sancho Reservoir	8	Several mines
91	147756	4144613	Odiel River	14	Several mines

Nº: Sampling point code (see Fig. 1 for location); **n:** number of samples taken

Table 2. Statistic parameters of 24 un-contaminated stream waters of the Odiel River Basin (total number of samples = 54)

	Mean	**Min**	**Max**	**SD**		**Mean**	**Min**	**Max**	**SD**
pH	7.22	5.77	9.00	0.85	Al (mg/L)	<dl	<dl	0.89	0.20
Eh (mV)	403	330	480	43.6	As (µg/L)	<dl	<dl	7.85	2.45
EC (µS/cm)	262	115	553	97.6	Be (µg/L)	<dl	<dl	<dl	0.24
DO (mg/L)	9.12	5.22	12.9	1.65	Cd (µg/L)	<dl	<dl	<dl	6.54
Ca (mg/L)	16.6	3.28	38.1	8.19	Co (µg/L)	<dl	<dl	<dl	6.41
K (mg/L)	1.50	0.20	4.38	0.79	Cr (µg/L)	<dl	<dl	<dl	0.74
Mg (mg/L)	10.6	1.61	20.7	4.77	Cu (mg/L)	0.04	<dl	0.20	0.07
Na (mg/L)	15.6	3.50	43.8	9.12	Fe (mg/L)	0.20	<dl	0.91	0.32
SiO_2 (mg/L)	5.62	<ld	20.4	2.57	Li (µg/L)	<dl	<dl	18.1	7.35
CO_3^{2-} (mg/L)	6.86	5.80	7.92	1.50	Mn (mg/L)	0.07	<dl	0.33	0.08
HCO_3^- (mg/L)	90.6	13.8	212	40.4	Mo (µg/L)	<dl	<dl	7.01	1.29
F (mg/L)	0.08	<dl	1.05	0.16	Ni (µg/L)	<dl	<dl	15.0	4.94
Cl (mg/L)	22.6	7.02	77.8	17.0	Pb (µg/L)	<dl	<dl	23.6	6.41
NO_2^- (mg/L)	0.04	<dl	0.42	0.09	Se (µg/L)	<dl	<dl	5.20	1.07
NO_3^- (mg/L)	1.53	<dl	6.96	1.93	Sn (µg/L)	<dl	<dl	<dl	3.63
SO_4^{2-} (mg/L)	29.9	8.70	75.9	18.1	Sr (µg/L)	71.1	3.22	516	74.3
PO_4^{3-} (mg/L)	212	<dl	1059	347	Zn (mg/L)	0.14	<dl	0.66	0.22

SD: standard deviation ; **<dl :** below detection limit; **EC:** specific conductance;
DO: dissolved oxygen

Table 3. Correlation matrix calculated using Spearman coefficients for the uncontaminated streams of the Odiel River Basin. (n = 44, bold values indicate $p<0.05$).

	Ca^{2+}	K^{+}	Mg^{2+}	Na^{+}	HCO_3^{-}	Cl^{-}	SO_4^{2-}
Ca^{2+}	1						
K^{+}	**0.39**	1					
Mg^{2+}	**0.71**	**0.52**	1				
Na^{+}	**0.57**	**0.47**	**0.84**	1			
HCO_3^{-}	**0.76**	0.05	**0.43**	0.26	1		
Cl^{-}	**0.45**	**0.39**	**0.82**	**0.88**	0.21	1	
SO_4^{2-}	0.27	**0.34**	**0.62**	**0.61**	-0.01	**0.61**	1

Table 4. Average values of the contaminant load transported by the Tinto and Odiel rivers (Olías et al., 2006) and comparison of the contribution with global riverine flux estimations of Gaillardet el al (2003) for the trace elements and of Meybeck (2003) for anthropogenic sulphate.

	Tinto (t/yr)	**Odiel** (t/yr)	**Total** (t/yr)	**Global gross flux** (Kt/yr)	**Tinto** (%)	**Odiel** (%)	**Total fraction** (%)
SO_4^{2-}	36589	147213	183802	124000	0.03	0.12	0.15
As	12	23	35	23	0.05	0.10	0.15
Cd	4	7	11	3	0.13	0.23	0.37
Cu	469	1252	1721	55	0.85	2.28	3.13
Fe	5075	2847	7922	2470	0.21	0.12	0.32
Mn	163	1452	1615	1270	0.01	0.11	0.13
Pb	15	12	27	3	0.50	0.40	0.90
Zn	863	2612	3475	23	3.75	11.4	15.1
Al	1224	4557	5781	1200	0.10	0.38	0.48
Co	9	62	71	5.5	0.16	1.13	1.29
Ni	2	34	36	30	0.01	0.11	0.12

Table 5. Statistical values of the measured parameters of the contaminated streams (total number of measured samples = 424)

	Mean	**Min**	**Max**	**SD**		**Mean**	**Min**	**Max**	**SD**
pH	3.65	2.05	8.59	1.2	Mg (mg/L)	227	1.17	2929	441
Eh (mV)	625	211	813	117	Mn (mg/L)	27.6	<dl	374	49.1
EC (mS/cm)	2.95	0.16	18.5	3.46	Na (mg/L)	20.8	<dl	107	14.1
DO (mg/L)	8.4	1.5	13.4	1.98	Ni (µg/L)	664	<dl	14429	1520
Al (mg/L)	135	<dl	2045	261	Pb (µg/L)	181	<dl	5930	455
As (µg/L)	242	<dl	7466	759	Sb (µg/L)	41.3	<dl	1041	113
Be (µg/L)	6.81	<dl	103	14.5	Se (µg/L)	49.4	<dl	1290	136
Ca (mg/L)	95.6	1.33	1123	120	Si (mg/L)	13.2	<dl	73.9	14.6
Cd (µg/L)	158	<dl	2249	300	Sn (µg/L)	57.6	<dl	1019	121
Co (µg/L)	1194	<dl	30869	2789	Sr (µg/L)	466	<dl	24203	1639
Cr (µg/L)	29.4	<dl	926	80.1	Zn (mg/L)	56.1	<dl	860	109
Cu (mg/L)	16.3	<dl	321	33.9	HCO_3^- (mg/L)	21.5	<dl	97.1	25.1
Fe_t (mg/L)	231	<dl	4282	509	F (mg/L)	0.76	<dl	11.4	1.93
Fe^{2+} (mg/L)	156	<dl	4000	442	Cl (mg/L)	18.2	2.83	64.4	11.2
K (mg/L)	1.66	<dl	11	1.38	NO_3^- (mg/L)	2.02	<dl	20.6	3.43
Li (µg/L)	261	<dl	3147	459	SO_4^{2-} (mg/L)	2685	11.1	36397	4727

SD: standard deviation ; **<dl :** below detection limit; **EC:** specific conductance;
DO: dissolved oxygen

Table 6. Representative selection of samples belonging to four groups of polluted streams

Code	Date	pH	Eh	EC	DO	SO_4^{2-}	Al	Ca	Cu	Fe^{+2}	Fe^{+3}	K	Mg	Mn	Na	Si	Zn	As	Be	Cd	Co	Cr	Li	Mo	Ni	Pb	Sb	Sn	Sr
			mV	mS/cm	%sat	mg/l												µg/l											
Type I																													
8	Dec02	2.05	658	6.08	42.0	5690	232	53.3	122	1300	30.0	2.16	46.5	5.80	13.5	16.2	55.0	4686	9.53	350	1120	17.2	153	47.7	116	106	<dl	354	1231
58	Jan04	2.50	675	4.50	32.0	4010	225	29.3	0.84	865	74.2	0.37	120	6.69	10.3	7.32	0.68	130	<dl	81.1	1080	19.6	113	56.6	65.7	175	143	<dl	87.5
62	Jan04	2.70	651	5.40	60.0	4099	160	202	16.2	865	47.6	2.65	197	45.3	21.4	11.7	24.9	356	9.34	138	746	19.6	437	46.8	576	202	136	<dl	147
40	Jan04	2.80	673	4.30	28.0	2411	54.0	135	10.2	456	64.3	<dl	90.0	40.2	19.0	22.3	53.2	1323	7.32	103	1130	23.0	380	20.2	713	203	<dl	250	1070
58	May04	2.58	676	8.48	26.3	13783	756	110	3.65	3178	773	<dl	385	22.2	25.9	41.4	3.97	157	6.72	379	3321	105	341	144	196	415	295	219	373
Type II																													
78	Jan04	2.80	777	2.65	98.8	1557	81.6	36.9	38.8	39.0	191	0.60	60.8	7.09	13.1	5.82	4.08	421	<dl	24.7	957	51.1	116	19.3	317	146	42.6	<dl	86.6
82	Jan04	2.90	781	3.50	96.3	2625	186	67.0	30.4	20.0	116	0.61	165	39.2	20.6	5.09	18.3	62.7	6.14	99.8	1511	36.2	361	35.9	887	261	71.1	8.45	112
78	Mar04	2.92	813	2.38	97.7	1443	84.9	31.1	27.6	7.00	153	0.42	67.6	9.39	17.1	15.3	3.61	220	<dl	22.8	860	47.6	130	10.2	327	114	5.93	8.14	79.8
82	Mar04	2.91	785	3.05	95.0	1217	94.4	30.2	12.4	5.00	45.1	<dl	74.8	21.0	11.7	5.50	7.18	<dl	<dl	44.1	749	<dl	143	<dl	421	75.1	<dl	<dl	37.9
78	May04	2.87	776	3.20	103	2278	127	58.4	40.8	20.0	142	0.63	133	15.9	23.8	26.0	8.14	102	3.99	22.8	1341	74.8	262	28.9	555	195	52.2	25.0	146
Type III																													
85	Jan04	3.55	742	1.42	76.5	861	84.1	39.1	10.1	3.00	9.95	1.69	88.3	16.0	29.5	2.64	7.90	<dl	6.23	37.3	607	<dl	173	<dl	353	185	<dl	5.13	44.1
26	Mar04	3.62	655	1.34	94.7	758	26.6	58.4	2.70	25.0	16.1	0.59	62.1	9.76	14.8	4.92	76.4	8.92	4.63	126	188	<dl	86.8	<dl	196	151	<dl	<dl	123
26	May04	3.18	662	2.59	87.2	1799	48.7	134	4.20	100	22.0	0.77	133	18.2	18.0	25.2	182	<dl	11.8	263	486	7.87	202	12.5	453	160	32.1	9.96	230
88	May04	2.81	720	2.44	82.5	1399	86.4	56.7	12.8	7.00	7.43	3.30	111	16.2	51.4	20.6	28.2	<dl	3.54	57.2	1044	27.3	170	16.5	459	128	31.3	10.2	171
34	Jan06	3.38	655	1.35	96.6	903	57.0	50.0	6.70	4.20	0.15	2.59	90.0	11.0	18.0	7.80	14.0		<dl	68.0	359	<dl	108	<dl	215	<dl	<dl	<dl	121
Type IV																													
11	Mar02	6.60	425	0.25	96.0	88.3	0.99	18.3	0.37	5.97	<dl	1.61	11.9	0.40	9.09	0.44	1.12	18.9	<dl	5.48	40.0	<dl	15.5	<dl	8.27	9.04	<dl	37.0	48.9
43	Apr03	3.92	591	1.01	83.0	565	31.5	53.1	3.81	2.50	0.62	2.00	47.9	5.01	16.7	8.45	6.37	25.5	<dl	37.2	190	<dl	74.8	<dl	87.3	9.18	<dl		77.4
34	Feb04	3.81	615	1.02	97.4	501	38.7	35.3	6.40	6.30	1.19	2.05	52.5	6.13	12.5	7.64	11.1	5.39	<dl	43.0	232	<dl	64.0	6.40	96.2	12.9	7.46	<dl	54.3
77	Jan06	4.05	591	0.69	89.0	327	14.0	32.0	1.80	1.81	<dl	2.00	40.0	2.80	24.0	8.40	5.40	9.70	<dl	13.0	90.0	<dl	29.0	<dl	54.0	<dl	<dl	11.0	96.0
88	Jan06	4.43	545	0.76	96.4	354	16.0	31.0	2.50	1.88	0.05	3.90	43.0	3.50	35.0	6.40	5.50		<dl	13.0	246	<dl	26.0	<dl	115	<dl	<dl	6.00	93.0

EC: specific conductance; **DO:** dissolved oxygen; **<dl:** below detection limit.

Table 7. Statistical data of contaminated waters in the hydrological year 2003/2004. The units are mg/L for Al, Ca, Cu, Fe, Fe2+, K, Mg, Mn, Na, Si, Zn and anions, µg/L for the rest of elements, mV for Eh and mS/cm for specific conductance. (**SD:** Standard deviation; **n:** number of samples). Rainfall accumulated in 30 days previous to every sampling; **<dl:** below detection limit).

	pH	Eh	CE	Al	Ca	Cu	Fe_t	Fe^{+2}	K	Mg	Mn	Na	Si	Zn	F	Cl	NO_3	SO_4	As	Cd	Co	Cr	Li	Ni	Pb	Sb	Se	Sn
Sampling Nov-03 (n=56) (Accumulated rainfall: 183 mm)																												
Mean	3.9	601	2.33	91.4	62.4	14.5	133	122	1.03	152	19.5	13.0	8.16	33.3	0.12	22.4	3.37	1946	249	149	955	28.6	114	542	664	6.41	8.95	
Max	7.3	769	13.7	1139	373	192	1528	1300	4.79	1465	179	49.6	44.2	402	0.22	50.1	5.38	18948	2765	1446	15761	477	936	6839	5930	134	137	<dl
Min	2.5	286	0.21	<dl	2.70	0.20	0.8	0.89	<dl	3.51	<dl	3.15	0.45	0.67	<dl	9.52	0.64	31.9	<dl	17.5	17.7	<dl	17.4	14.5	<dl	<dl	<dl	<dl
SD	1.2	119	3.04	240	88.7	36.6	292	284	1.01	335	42.6	9.48	9.21	82.9	0.1	14.3	1.53	4221	687	331	2783	82.2	216	1353	1180	23.0	26.4	
Sampling Jan-04 (n=43) (Accumulated rainfall: 20 mm)																												
Mean	3.7	629	2.65	118	79.2	17.2	250	204	1.20	201	25.4	17.3	5.77	44.7	0.14	14.7	0.81	2415	374	134	1116	35.6	225	613	139	74.3		2.36
Max	6.9	781	13.3	952	325	151	2003	1756	4.17	1985	220	46.0	26.0	345	0.24	23.0	1.67	19332	7466	1277	11733	417	1807	4738	741	625	<dl	22.2
Min	2.5	211	0.24	<dl	2.70	<dl	<dl	<dl	<dl	4.74	<dl	2.40	0.64	<dl	<dl	8.00	<dl	38.6	<dl	<dl	<dl	<dl	<dl	<dl	<dl	<dl	<dl	<dl
SD	1.1	124	3.04	218	92.1	32.8	451	427	0.88	408	46.1	9.34	7.03	88.8	0.1	5.16	0.52	4329	1312	270	2460	82.9	391	1303	195	150		3.95
Sampling Feb-04 (n=44) (Accumulated rainfall: 204 mm)																												
Mean	4.3	576	1.35	44.9	42.2	6.79	64.1	55.2	1.45	65.1	9.01	12.3	4.63	17.7	0.17	14.7	2.02	729	189	47.1	370	16.7	80.9	157	50.0	14.0	14.6	3.70
Max	8.6	714	8.23	524	376	76.5	941	845	5.21	679	90.1	37.2	19.8	198	0.38	45.8	5.24	6399	3487	563	6091	420	1065	2024	721	159	162	46.1
Min	2.5	282	0.16	<dl	1.33	<dl	<dl	<dl	0.38	1.17	<dl	2.12	<dl	<dl	<dl	2.83	0.20	11.1	<dl	<dl	<dl	<dl	<dl	<dl	<dl	<dl	<dl	<dl
SD	1.3	119	1.88	112	74.7	16.0	168	151	1.11	142	19.6	8.53	4.52	43.9	0.1	11.9	1.84	1506	610	119	1065	72.0	199	424	128	35.8	36.3	10.3
Sampling Mar-04 (n=44) (Accumulated rainfall: 52 mm)																												
Mean	4.0	612	2.24	96.3	83.6	11.1	145	103	1.25	134	19.0	19.0	9.00	27.9	0.19	18.4	1.32	1826	178	92.4	784	19.1	172	446	76.7	25.7	26.4	9.80
Max	7.1	813	11.4	827	1125	98.9	1243	1090	4.02	1281	158	46.8	29.4	248	0.39	36.8	6.92	13401	3006	856	9207	290	1519	3980	673	383	221	78.6
Min	2.6	259	0.24	<dl	2.99	<dl	<dl	<dl	<dl	4.36	<dl	5.82	1.21	<dl	<dl	7.75	<dl	34.9	<dl	<dl	<dl	<dl	<dl	<dl	<dl	<dl	<dl	<dl
SD	1.3	125	2.61	190	185	21.2	302	260	0.99	263	34.7	9.25	5.65	59.2	0.12	10.0	2.29	3126	597	186	1817	53.1	315	992	126	70.9	55.2	18.9
Sampling May-04 (n=44) (Accumulated rainfall: 59 mm)																												
Mean	3.6	617	2.87	152	96.9	18.0	331	266	1.46	221	28.8	25.1	19.8	50.1	0.16	16.1	0.16	3047	144	155	1260	33.4	303	661	135	65.0	93.1	31.0
Max	7.0	776	13.0	1269	346	164	3951	3178	3.73	1745	221	51.4	57.2	421	0.35	25.0	0.26	18816	2312	1371	14478	446	2413	6315	618	440	644	220
Min	2.6	274	0.20	0.88	10.9	<dl	<dl	<dl	<dl	6.29	<dl	8.28	4.01	0.11	<dl	8.41	<dl	53.8	<dl	<dl	<dl	<dl	<dl	<dl	3.40	<dl	<dl	<dl
SD	1.2	132	3.15	287	87.4	33.9	801	672	0.91	380	48.6	11.4	14.6	98.9	0.11	7.01	0.1	4981	513	295	2705	79.2	512	1347	156	110	160	61.4
Sampling Jun-04 (n=26) (Accumulated rainfall: 4.8 mm)																												
Mean	3.1	653	5.04	286	187	37.5	572	403	1.64	553	62.4	26.7	11.0	126	<dl	9.10	<dl	5988	223	336	3038	82.1	534	1614	296	157	189	70.7
Max	7.3	748	18.5	2045	569	321	4282	4000	4.45	2929	374	69.1	62.8	860	<dl	9.10	<dl	36397	3817	2249	30869	926	3147	14429	1430	1041	1290	496
Min	2.1	417	0.20	<dl	11.3	<dl	<dl	<dl	0.39	5.77	<dl	7.46	1.97	0.73	<dl	9.10	<dl	41.1	<dl	<dl	<dl	<dl	5.83	<dl	5.95	<dl	<dl	<dl
SD	1.1	82	4.99	488	160	71.4	1015	885	1.23	832	93.3	17.2	13.0	203				8618	808	542	6726	195	799	3342	331	250	308	115
Sampling Aug-04 (n=23) (Accumulated rainfall: 0.0 mm)																												
Mean	3.0	699	6.00	344	215	38.3	459		2.52	636	75.9	41.0	42.2	148	<dl	17.3	<dl	6892	285	445	2829	52.7	731	1862	364	150	200	86.2
Max	7.3	795	15.8	1614	454	140	1774		7.72	2769	296	107	73.2	584	<dl	24.6	<dl	24155	2210	1605	12459	240	3117	8733	1501	542	813	377
Min	2.2	395	0.21	0.30	14.4	<dl	<dl		1.06	8.33	<dl	10.2	4.24	0.97	<dl	9.89	<dl	62.6	<dl	<dl	<dl	<dl	6.34	<dl	3.86	6.80	<dl	<dl
SD	1.0	104	4.92	423	133	42.5	523		1.45	816	79.0	26.1	18.2	165		10.4		7658	529	480	3574	65.8	780	2502	334	157	221	103

Table 8. Analytical data for three sampling points during the studied period (shadowed data belong to the same hydrological year).

Date	pp	pH	Eh	EC	DO	SO_4^{2-}	Zn	Al	Ca	Cu	Fe	Fe^{+2}	Fe^{+3}	K	Mg	Mn	Na	Si	As	Cd	Co	Cr	Li	Mo	Ni	Pb	Sb	Sn	Sr
	mm		mV	mS/cm	%sat	mg/l													µg/l										
Sample S15 (Upper basin)																													
Feb02	56.0	3.58	na	1.12	na	993	11.0	53.8	66.5	2.65	31.9	na	na	2.10	75.9	10.9	23.3	3.26	21.1	63.5	350	4.65	121	7.32	163	14.0	<dl	111	1946
Mar02	45.2	4.01	na	0.87	na	612	4.29	29.5	59.4	1.48	21.5	na	na	1.99	44.2	5.74	20.2	2.23	18.5	50.5	214	4.15	67.1	8.32	131	22.2	<dl	113	1274
Jun03	18.0	3.17	620	1.95	na	1374	23.0	163	60.3	7.88	12.3	na	na	1.23	154	19.9	15.2	9.33	4.71	113	639	4.71	225	9.88	301	10.1	<dl	113	2330
Jul03	0.0	2.76	685	5.71	na	4456	66.4	394	125	19.5	149	16.2	132	2.08	386	57.3	29.6	17.0	9.08	301	1856	15.2	628	17.8	720	42.0	<dl	347	3008
Nov03	183	4.24	576	0.88	100	229	3.87	11.5	11.2	2.28	1.95	1.56	0.39	0.33	20.8	2.27	4.73	2.91	<dl	35.4	98.3	<dl	24.2	<dl	55.8	<dl	<dl	na	78.9
Jan04	20.0	3.30	673	1.60	96.7	295	5.25	18.0	18.8	3.67	6.24	na	na	0.45	21.1	3.48	2.40	2.02	<dl	24.8	132	<dl	9.99	<dl	58.7	8.35	<dl	<dl	29.0
Feb04	204	3.82	617	0.80	97.8	358	6.29	27.9	26.3	4.52	10.3	10.0	0.27	1.71	34.1	3.86	9.33	5.56	8.33	28.2	145	<dl	38.1	<dl	57.2	10.4	<dl	<dl	44.6
Mar04	52.0	4.49	586	1.10	96.2	545	9.15	36.6	28.7	4.16	6.60	5.00	1.60	2.16	52.1	7.00	11.8	7.50	<dl	36.6	197	<dl	58.9	<dl	109	<dl	<dl	<dl	62.5
May04	59.0	3.66	589	1.51	96.0	1048	16.4	54.2	59.5	8.05	11.6	10.0	1.59	1.32	96.1	11.3	17.5	8.61	<dl	63.0	391	<dl	120	12.2	195	32.2	24.5	7.06	109
Jun04	4.8	2.81	663	3.87	97.5	2692	40.9	157	139	20.9	83.6	58.0	25.6	1.70	234	28.2	21.7	5.42	<dl	169	1023	15.2	269	33.2	480	108	51.1	25.6	259
Jul04	0.0	2.39	na	8.01	na	8498	138	535	258	70.4	213	2.30	211	2.43	840	111	53.7	46.5	12.4	700	3954	44.1	894	95.9	2006	247	152	59.0	493
Aug04	0.0	2.64	757	8.73	102	9079	145	616	267	75.5	271	na	na	3.39	774	104	70.4	41.4	141	604	3684	38.9	1087	164	1770	375	231	133	456
Oct04	149	2.97	690	3.93	na	3238	58.5	281	106	29.9	97.5	21.5	76.0	2.34	308	36.4	28.9	15.4	6.71	245	1251	5.79	451	18.2	539	19.6	na	<dl	210
Oct05	84.8	2.75	690	4.38	na	na	na	na	na	na	104	68.5	35.7	na	na	na	na	na	101	na	na	na	na	na	na	na	na	na	na
Jan06	69.0	3.40	680	1.63	95.2	1137	20.0	77.0	57.0	9.10	13.9	12.6	1.25	3.02	118	15.0	16.0	9.00	na	95.0	475	7.00	138	<dl	281	32.5	<dl	<dl	126
Apr06	48.8	3.07	765	2.23	85.2	1578	27.0	102	61.0	14.0	36.0	8.38	27.6	4.80	156	18.0	16.0	10.0	na	121	630	9.60	210	<dl	334	<dl	<dl	<dl	140
Sample S45 (Middle basin)																													
Feb02	61.0	4.07	na	0.71	na	435	6.48	21.9	37.7	3.66	8.69	na	na	1.90	42.1	5.00	14.5	0.47	14.1	31.0	161	<dl	42.9	<dl	75.7	18.3	<dl	35.7	74.5
Apr03	79.6	3.61	623	1.07	na	700	9.99	31.5	44.3	7.22	10.6	na	na	1.97	50.1	7.09	12.8	8.03	16.0	48.6	224	4.01	48.8	<dl	131	40.4	<dl	36.6	75.3
Jun03	18.2	3.28	708	1.58	na	1398	19.6	80.3	57.4	13.5	9.13	na	na	1.94	114	21.4	14.0	10.6	<dl	97.4	475	4.37	96.6	<dl	256	54.8	6.10	36.0	100
Jul03	0.0	2.94	696	3.24	na	2091	23.5	153	104	6.48	10.8	6.10	4.70	2.04	174	27.7	24.7	18.0	7.21	126	777	9.85	301	19.0	326	143	<dl	223	2305
Nov03	183	4.67	531	0.51	91.0	323	5.11	9.43	29.8	2.53	3.25	na	na	1.35	30.3	3.13	11.1	4.83	<dl	37.1	115	<dl	28.8	<dl	60.6	143	<dl	na	120
Jan04	20.0	3.65	637	1.14	na	451	7.78	26.5	30.6	4.86	5.52	5.00	0.52	0.80	39.5	5.12	9.95	1.85	<dl	31.9	178	<dl	42.7	<dl	89.3	20.4	<dl	<dl	59.4
Feb04	204	3.82	619	1.01	88.7	561	12.2	41.4	36.8	7.16	8.49	8.00	0.49	5.21	56.8	6.50	13.6	6.65	13.4	50.3	224	<dl	72.2	8.65	101	35.6	21.1	<dl	68.2
Mar04	52.0	3.66	588	1.10	96.6	764	11.6	44.8	37.1	5.95	9.81	8.50	1.31	1.51	67.4	8.82	16.3	8.13	10.7	48.3	268	<dl	80.2	6.70	137	18.2	7.34	5.86	88.1
May04	59.0	3.51	614	1.26	92.4	789	12.1	39.6	49.9	6.18	6.90	6.00	0.90	1.29	69.0	8.27	16.3	9.16	<dl	43.5	284	<dl	88.2	9.49	149	41.3	23.9	5.02	96.8
Jun04	4.8	2.72	707	2.66	101	2148	35.7	118	105	17.7	20.5	8.00	12.5	4.45	207	25.5	26.0	4.61	34.4	147	831	16.3	222	29.4	451	217	50.2	26.0	194
Jul04	0.0	2.17	na	3.05	na	2095	33.1	121	155	13.0	11.4	11.0	0.40	2.49	199	28.9	31.0	29.9	9.10	130	840	14.6	231	20.0	481	273	31.6	9.83	236
Aug04	0.0	2.93	781	3.47	84.6	2796	52.9	179	186	20.9	23.6	na	na	3.95	272	42.2	41.2	40.5	80.6	195	1250	33.3	331	66.0	662	493	99.7	69.1	312
Oct04	149	3.01	712	2.46	na	1590	25.7	127	90.0	11.4	25.8	8.02	17.8	5.55	153	20.6	22.8	11.5	4.52	106	602	<dl	205	<dl	270	95.1	na	<dl	160
Oct05	84.8	2.97	720	3.54	na	na	na	na	na	na	26.5	18.6	7.95	na	na	na	na	na	3217	na	na	na	na	na	na	na	na	na	na
Jan06	69.0	3.03	720	1.86	98.5	1194	25.0	78.0	67.0	9.80	23.9	20.5	3.39	2.80	119	18.0	21.0	9.90	30.2	96.0	526	19.0	153	<dl	281	52.0	<dl	10.0	147
Apr06	48.8	3.24	764	1.21	85.4	762	14.0	45.0	45.0	6.30	8.56	2.22	6.34	4.20	73.0	9.30	16.0	8.80	<dl	54.0	288	6.00	89.0	<dl	148	23.0	<dl	8.00	103
Sample S91 (Lower basin)																													
Jul03	0.0	3.85	517	0.73	na	na	4.32	8.19	na	1.75	1.21	1.21	<dl	na	na	2.43	na	na	<dl	16.0	133	<dl	na	na	55.0	19.0	na	na	85.0
Nov03	183	4.05	675	0.74	79.1	435	6.33	17.7	31.2	2.96	1.52	na	na	1.27	40.4	4.22	14.6	7.69	<dl	41.8	158	3.09	32.8	<dl	91.9	428	<dl	na	130
Jan04	20.0	3.92	665	1.05	67.5	572	9.73	34.0	37.6	4.31	6.09	3.00	3.09	1.36	54.0	5.79	20.3	3.90	5.39	26.2	204	<dl	61.4	<dl	103	20.0	13.6	<dl	77.0
Feb04	204	4.71	505	0.36	94.1	141	2.69	7.72	14.7	1.29	3.55	3.00	0.55	1.12	13.9	1.43	10.4	0.65	<dl	<dl	40.2	<dl	13.6	<dl	11.0	<dl	<dl	<dl	36.1
Mar04	52.0	3.79	602	0.93	95.0	556	8.85	30.8	37.2	3.86	2.72	2.50	0.22	1.17	52.6	6.29	18.1	7.56	4.82	32.3	193	<dl	58.8	<dl	103	14.9	<dl	<dl	88.0
May04	59.0	3.57	578	1.05	na	540	8.84	24.0	51.2	3.47	1.39	1.30	0.09	1.78	48.1	5.51	18.2	8.85	<dl	20.8	194	<dl	59.1	<dl	98.4	31.5	12.1	<dl	95.0
Jun04	4.8	3.38	689	1.54	93.4	927	14.4	44.9	70.6	6.18	1.15	0.80	0.35	2.06	84.8	10.1	23.6	19.9	<dl	47.1	331	<dl	108	9.19	166	71.4	<dl	<dl	135
Jul04	0.0	3.24	na	1.59	na	904	14.1	43.5	72.7	5.19	1.60	1.60	<dl	2.57	98.6	11.6	27.0	27.9	<dl	57.1	392	<dl	108	7.22	213	82.5	9.14	<dl	151
Aug04	0.0	3.35	607	1.66	104	1036	15.8	50.0	82.4	5.61	3.41	na	na	3.00	101	12.1	31.2	34.5	18.8	59.3	399	<dl	124	15.7	219	118	26.8	13.2	168
Oct04	149	3.18	726	2.21	na	1461	25.5	121	76.5	10.6	13.3	3.62	9.72	4.35	145	19.1	28.7	16.7	<dl	90.5	580	<dl	189	<dl	274	46.2	na	<dl	161
Oct05	84.8	3.42	540	1.22	na	na	na	na	na	na	1.92	1.92	<dl	na	na	na	na	na	7.32	na	na	na	na	na	na	na	na	na	na
Jan06	69.0	3.39	655	0.87	19.5	477	11.0	22.0	41.0	3.10	2.42	2.43	<dl	2.00	49.0	6.30	21.0	8.30	na	30.0	191	5.00	47.0	<dl	102	44.0	<dl	<dl	100
Apr06	48.8	3.41	682	1.11	91.4	471	8.80	24.0	36.0	3.70	2.09	1.61	0.49	2.50	46.0	5.40	18.0	9.90	na	30.0	176	3.60	55.0	<dl	90.0	73.0	<dl	<dl	91.0

EC: specific conductance; **DO:** dissolved oxygen; **pp:** accumulated rainfall; **<dl:** below detection limit; **na:** no analyzed

Figure 1

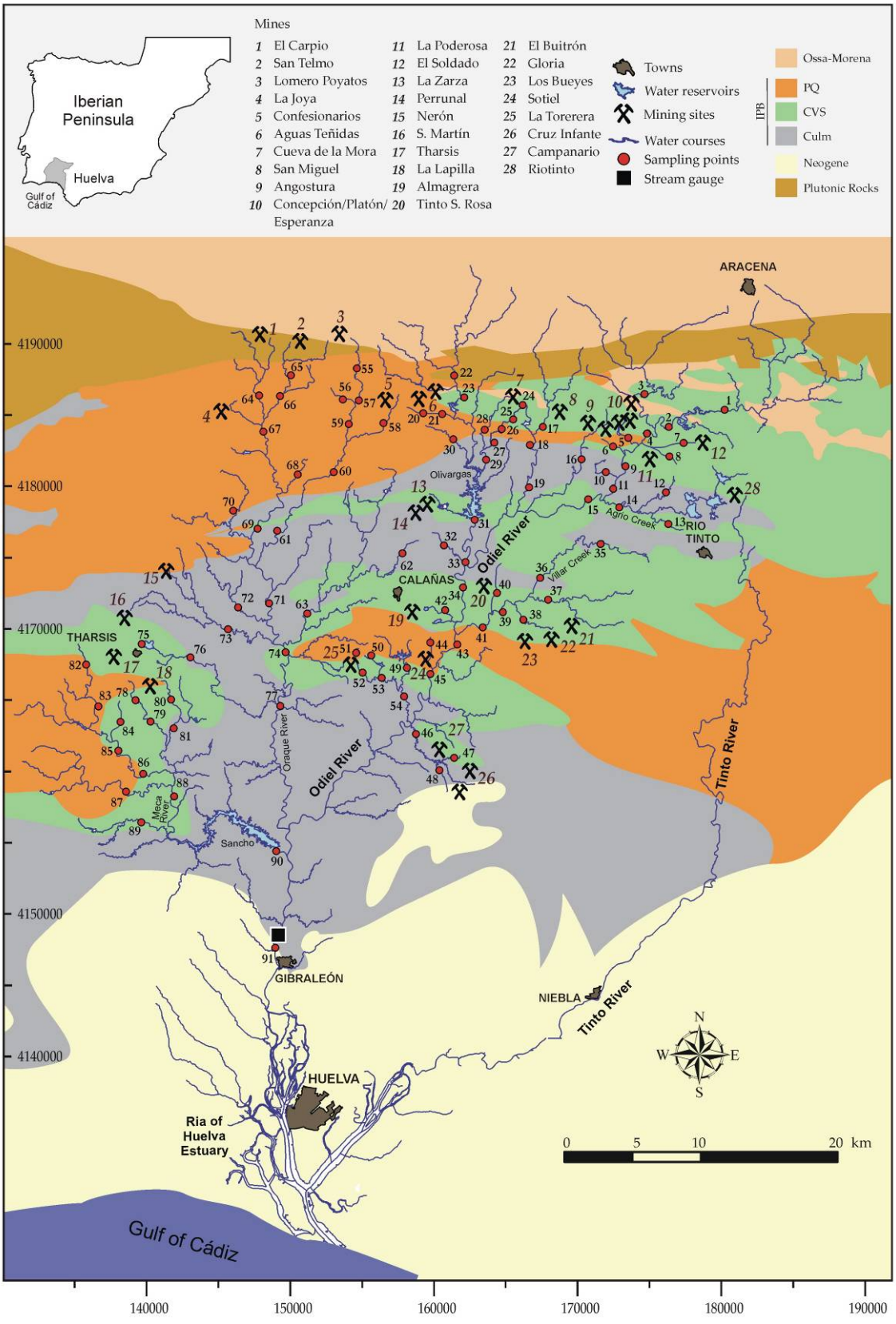
Iberian Peninsula
Huelva
Gulf of Cádiz
Mines
1 El Carpio
2 San Telmo
3 Lomero Poyatos
4 La Joya
5 Confesionarios
6 Aguas Teñidas
7 Cueva de la Mora
8 San Miguel
9 Angostura
10 Concepción/Platón/ Esperanza
11 La Poderosa
12 El Soldado
13 La Zarza
14 Perrunal
15 Nerón
16 S. Martín
17 Tharsis
18 La Lapilla
19 Almagrera
20 Tinto S. Rosa
21 El Buitrón
22 Gloria
23 Los Bueyes
24 Sotiel
25 La Torerera
26 Cruz Infante
27 Campanario
28 Riotinto
Towns
Water reservoirs
Mining sites
Water courses
Sampling points
Stream gauge
IPB
Ossa-Morena
PQ
CVS
Culm
Neogene
Plutonic Rocks
ARACENA
RIO TINTO
CALAÑAS
THARSIS
GIBRALEÓN
NIEBLA
HUELVA
Olivargas
Agro Creek
Villar Creek
Odiel River
Oraque River
Meca River
Sancho
Tinto River
Ria of Huelva Estuary
Gulf of Cádiz
N
W
E
S
0 5 10 20 km
4190000
4180000
4170000
4150000
4140000
140000
150000
160000
170000
180000
190000

Figure 2

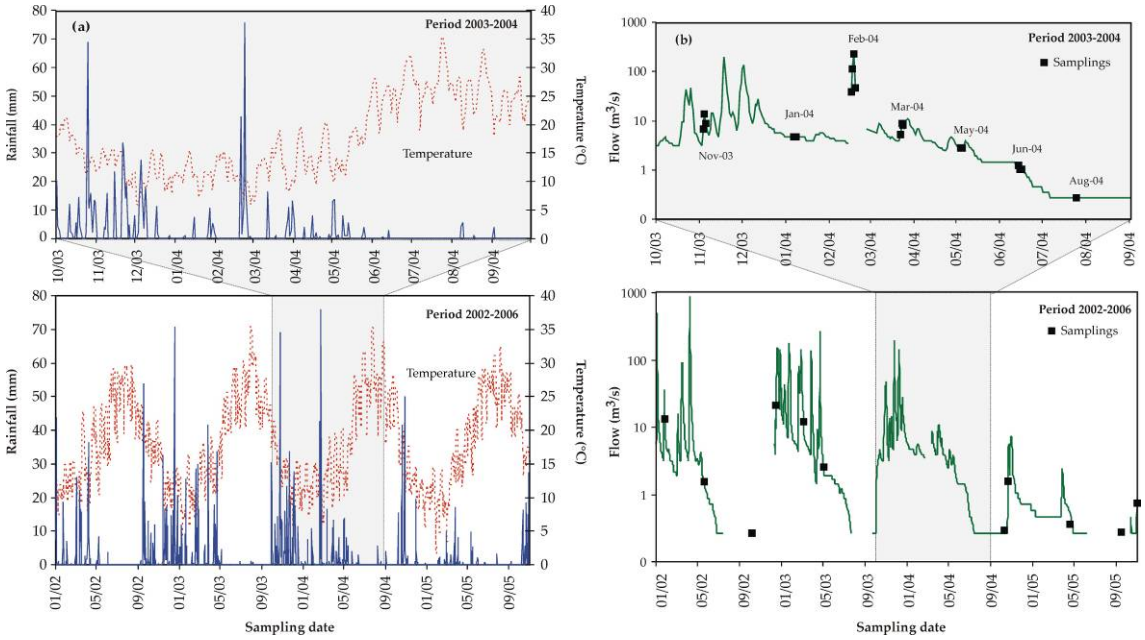
(a)
Period 2003-2004
Rainfall (mm)
Temperature (°C)
Temperature
Period 2002-2006
Sampling date
(b)
Period 2003-2004
Samplings
Flow (m³/s)
Nov-03
Jan-04
Feb-04
Mar-04
May-04
Jun-04
Aug-04
Period 2002-2006
Samplings
Sampling date

Figure 3

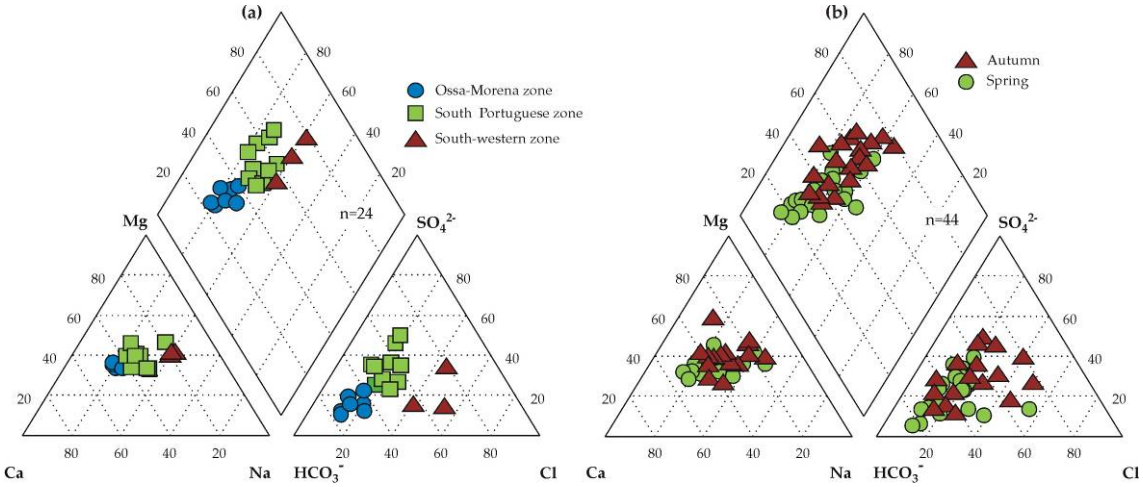
(a)
Ossa-Morena zone
South Portuguese zone
South-western zone
n=24
Mg
SO_4^{2-}
Ca
Na
HCO_3^-
Cl
(b)
Autumn
Spring
n=44
Mg
SO_4^{2-}
Ca
Na
HCO_3^-
Cl

Figure 4

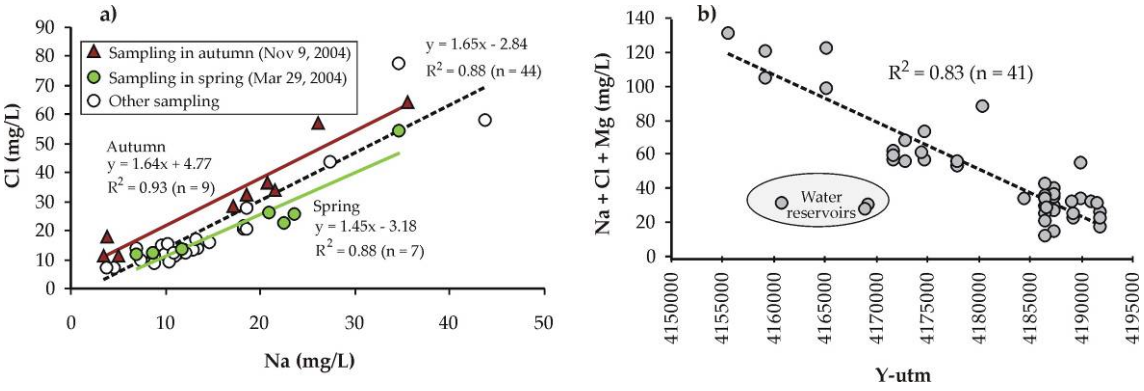
a)
Sampling in autumn (Nov 9, 2004)
Sampling in spring (Mar 29, 2004)
Other sampling
y = 1.65x - 2.84
R2 = 0.88 (n = 44)
Autumn
y = 1.64x + 4.77
R2 = 0.93 (n = 9)
Spring
y = 1.45x - 3.18
R2 = 0.88 (n = 7)
Cl (mg/L)
Na (mg/L)
b)
R2 = 0.83 (n = 41)
Water reservoirs
Na + Cl + Mg (mg/L)
Y-utm

Figure 5

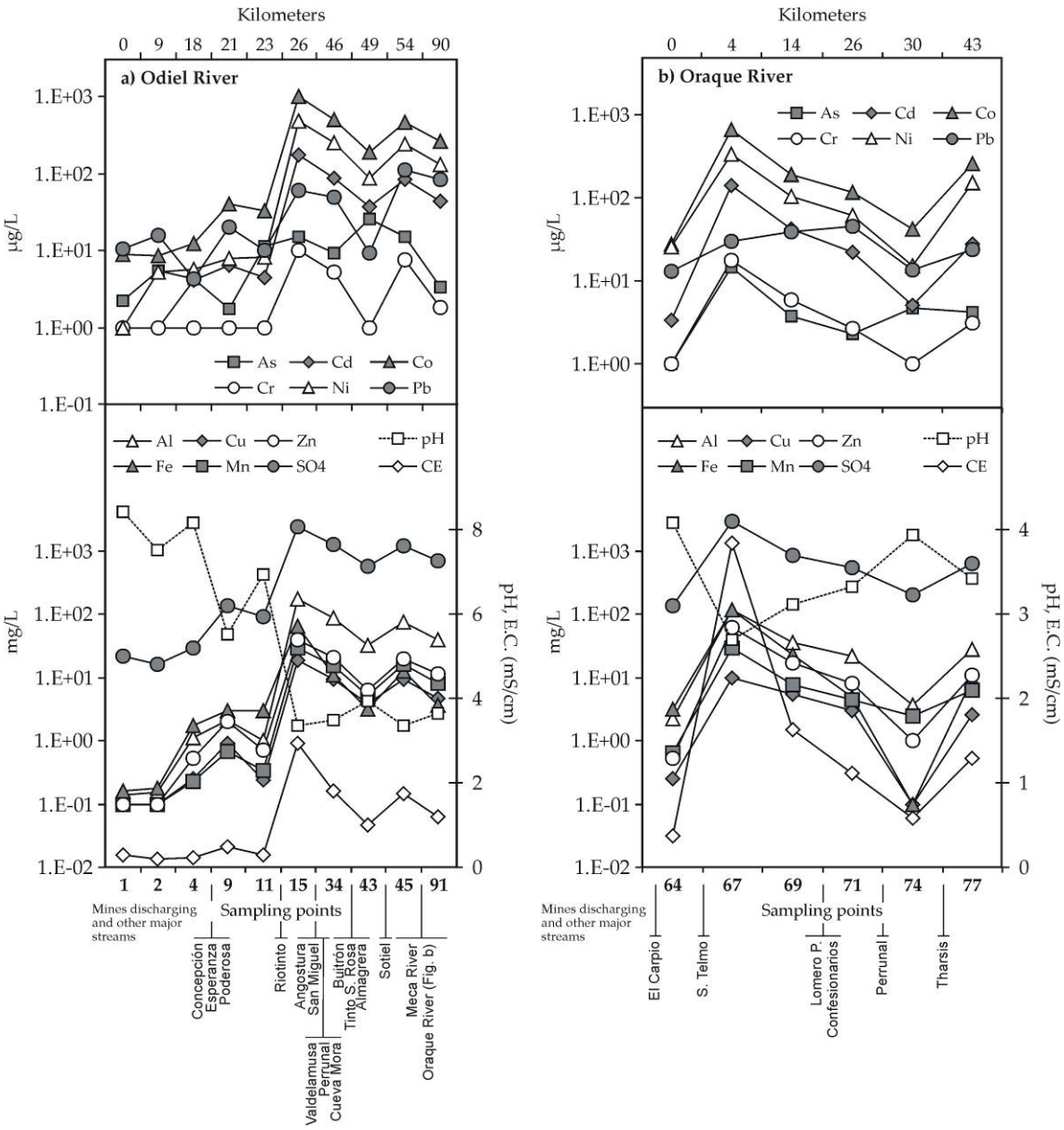
Kilometers
0 9 18 21 23 26 46 49 54 90
a) Odiel River
µg/L
1.E+03
1.E+02
1.E+01
1.E+00
1.E-01
As Cd Co
Cr Ni Pb
Al Cu Zn pH
Fe Mn SO4 CE
mg/L
1.E+03
1.E+02
1.E+01
1.E+00
1.E-01
1.E-02
pH, E.C. (mS/cm)
8
6
4
2
0
1 2 4 9 11 15 34 43 45 91
Mines discharging and other major streams
Sampling points
Concepcion
Esperanza
Poderosa
Riotinto
Angostura
San Miguel
Valdelamusa
Perrunal
Cueva Mora
Buitrón
Tinto
S. Rosa
Almagrera
Sotiel
Meca River
Oraque River (Fig. b)
Kilometers
0 4 14 26 30 43
b) Oraque River
As Cd Co
Cr Ni Pb
Al Cu Zn pH
Fe Mn SO4 CE
4
3
2
1
0
64 67 69 71 74 77
El Carpio
S. Telmo
Lomero P.
Confesionarios
Perrunal
Tharsis

Figure 6

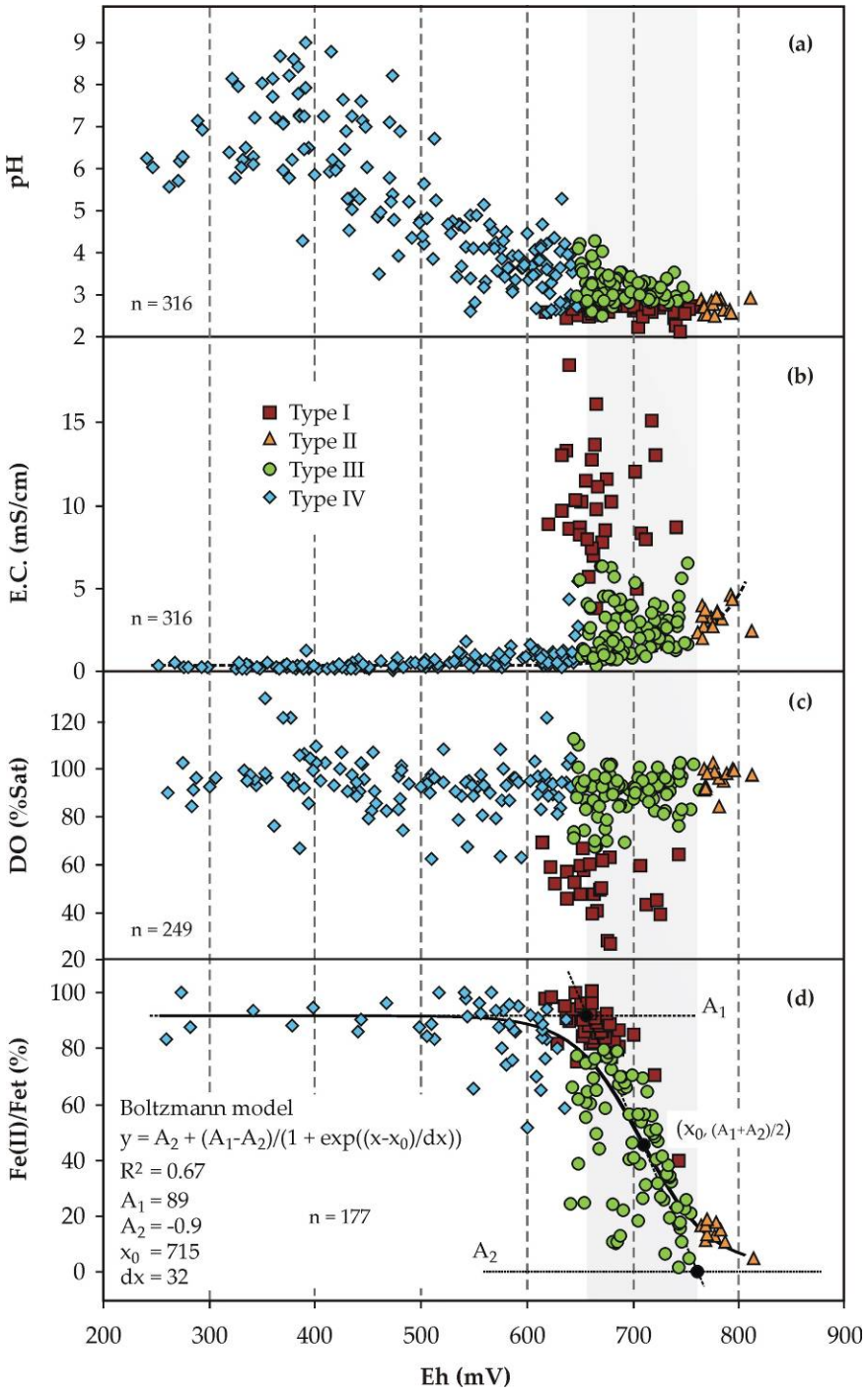
(a)
pH
n = 316
(b)
E.C. (mS/cm)
Type I
Type II
Type III
Type IV
n = 316
(c)
DO (%Sat)
n = 249
(d)
Fe(II)/Fet (%)
A1
A2
(x0, (A1+A2)/2)
Boltzmann model
y = A2 + (A1-A2)/(1 + exp((x-x0)/dx))
R2 = 0.67
A1 = 89
A2 = -0.9
x0 = 715
dx = 32
n = 177
Eh (mV)

Figure 7

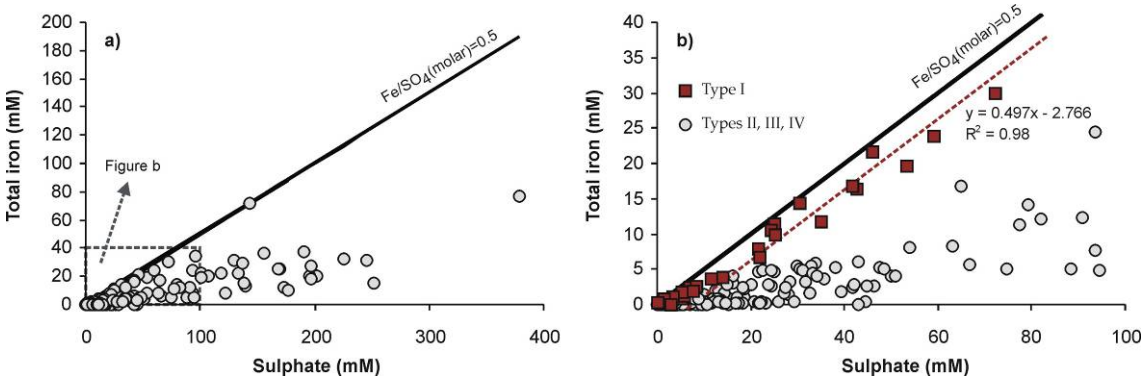
a)
Fe/SO4(molar)=0.5
Figure b
Total iron (mM)
Sulphate (mM)
b)
Type I
Types II, III, IV
y = 0.497x - 2.766
R2 = 0.98
Fe/SO4(molar)=0.5
Total iron (mM)
Sulphate (mM)

Figure 8

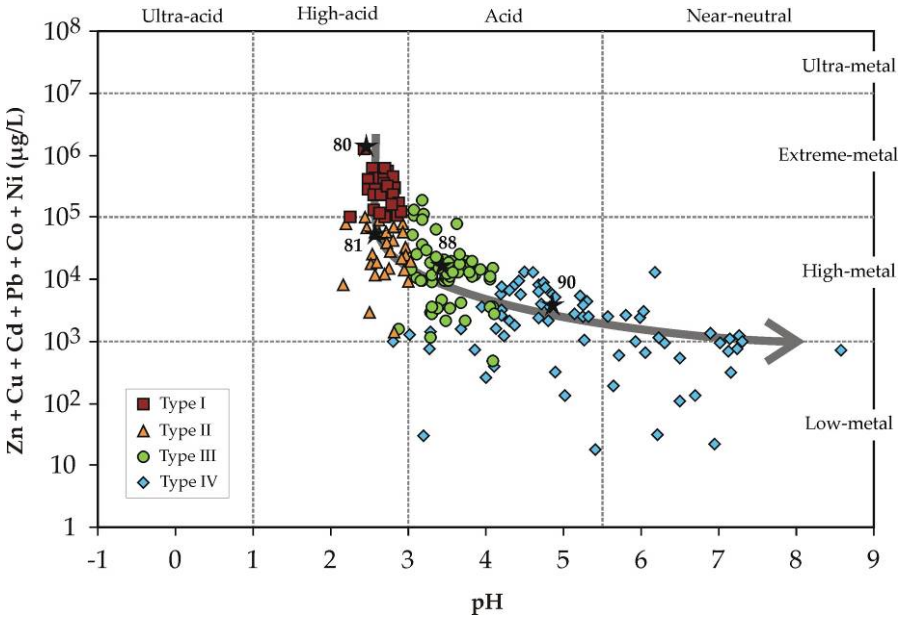
Ultra-acid
High-acid
Acid
Near-neutral
Ultra-metal
Extreme-metal
High-metal
Low-metal
80
81
88
90
Type I
Type II
Type III
Type IV
Zn + Cu + Cd + Pb + Co + Ni (µg/L)
pH

Figure 9

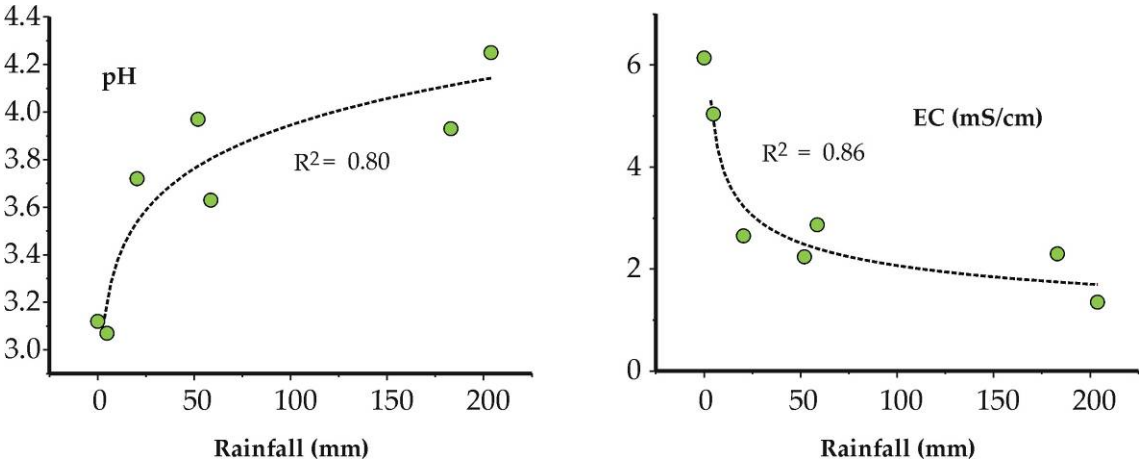
pH
R2= 0.80
4.4
4.2
4.0
3.8
3.6
3.4
3.2
3.0
0
50
100
150
200
Rainfall (mm)
EC (mS/cm)
R2 = 0.86
6
4
2
0
0
50
100
150
200
Rainfall (mm)

Figure 10

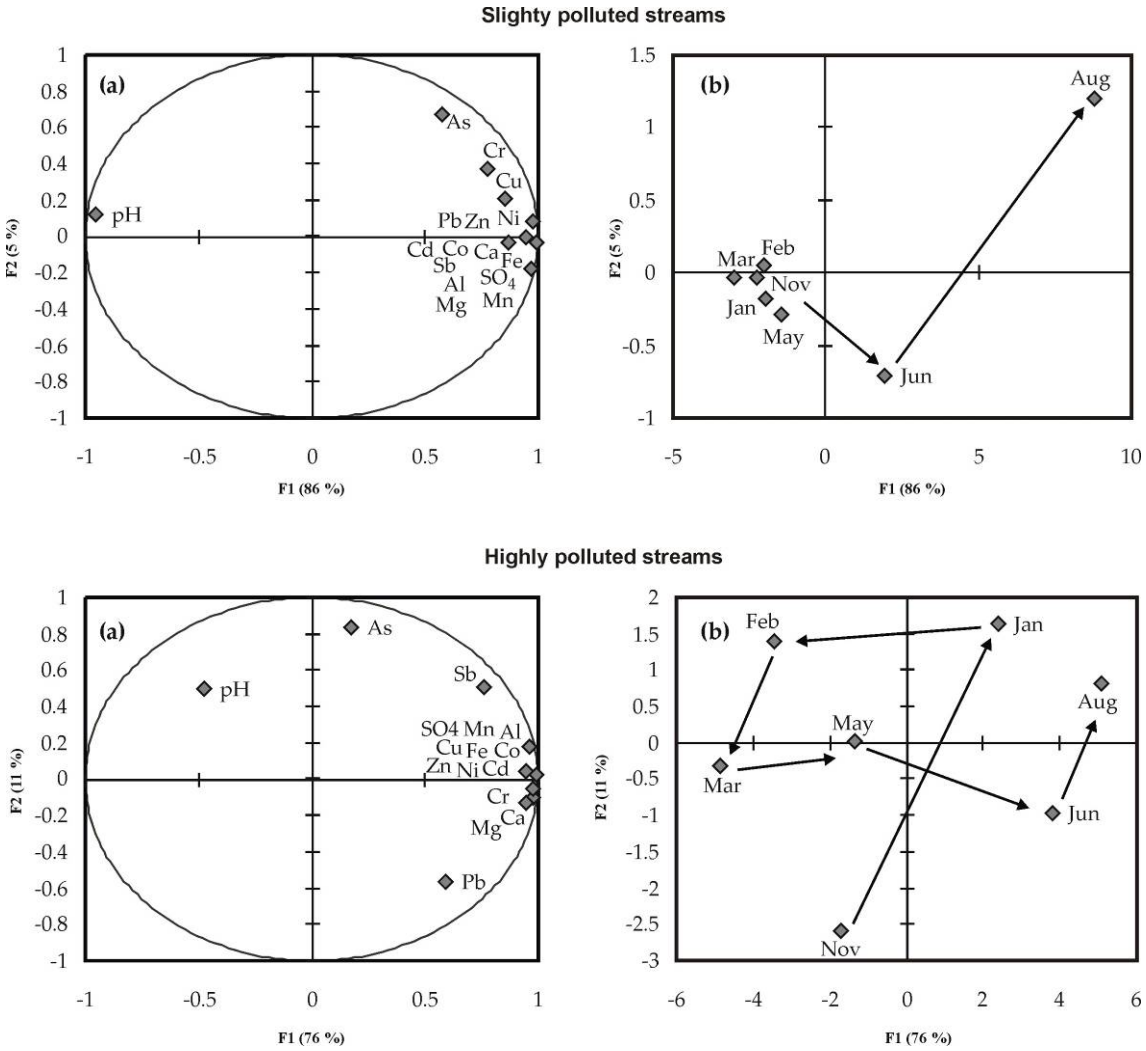
Slighty polluted streams
(a)
As
Cr
Cu
pH
Pb Zn Ni
Cd Co Ca Fe
Sb
Al SO4
Mg Mn
F2 (5 %)
F1 (86 %)
(b)
Aug
Feb
Mar
Nov
Jan
May
Jun
F2 (5 %)
F1 (86 %)
Highly polluted streams
(a)
As
pH
Sb
SO4 Mn Al
Cu Fe Co
Zn Ni Cd
Cr
Ca
Mg
Pb
F2 (11 %)
F1 (76 %)
(b)
Feb
Jan
Aug
May
Mar
Jun
Nov
F2 (11 %)
F1 (76 %)

Figure 11

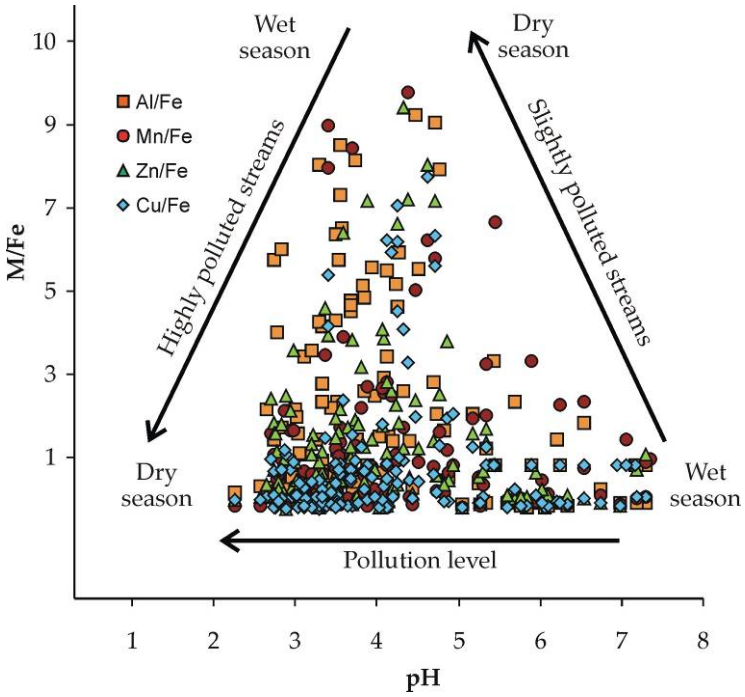
Wet
season
Dry
season
Al/Fe
Mn/Fe
Zn/Fe
Cu/Fe
Highly polluted streams
Slightly polluted streams
Dry
season
Wet
season
Pollution level
M/Fe
pH
10
9
7
5
3
1
1
2
3
4
5
6
7
8

Figure 12

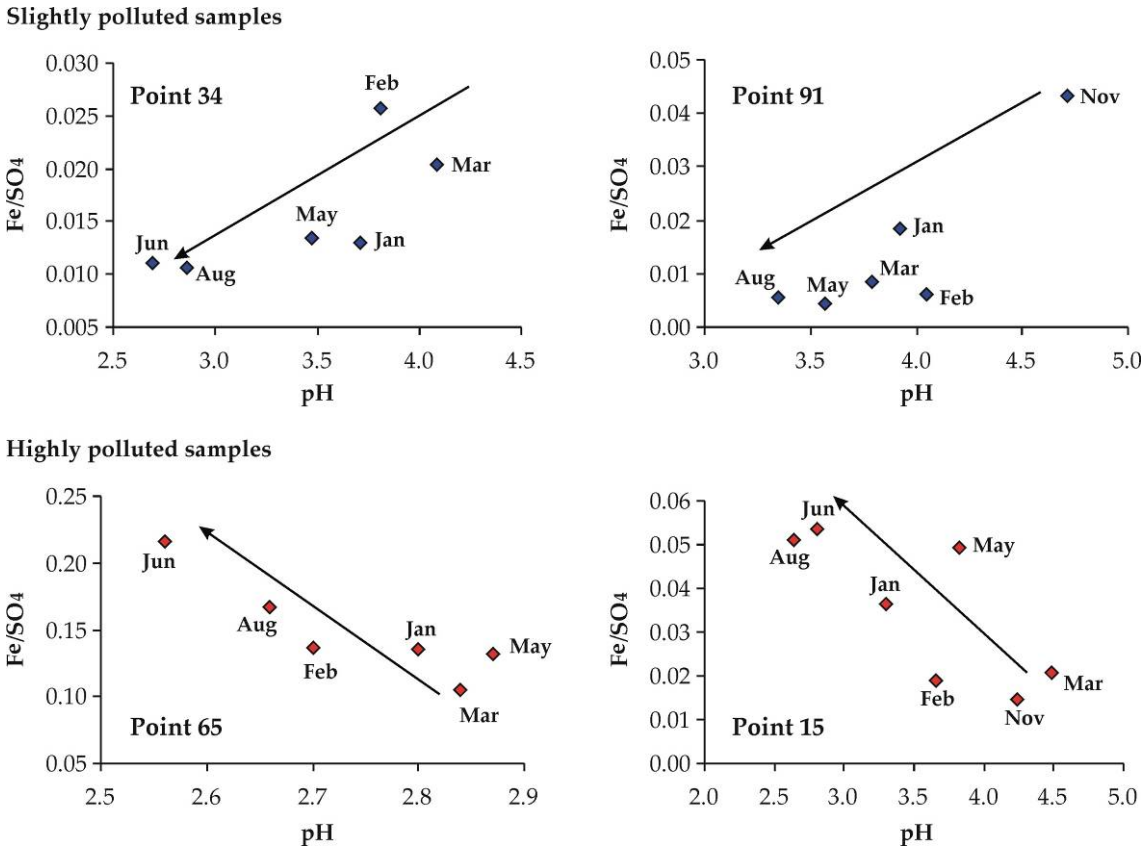
Slightly polluted samples
Point 34
Feb
Mar
May
Jan
Jun
Aug
Fe/SO4
pH
Point 91
Nov
Jan
Aug
May
Mar
Feb
Highly polluted samples
Point 65
Jun
Aug
Feb
Jan
May
Mar
Point 15
Jun
Aug
May
Jan
Feb
Nov
Mar

Figure 13

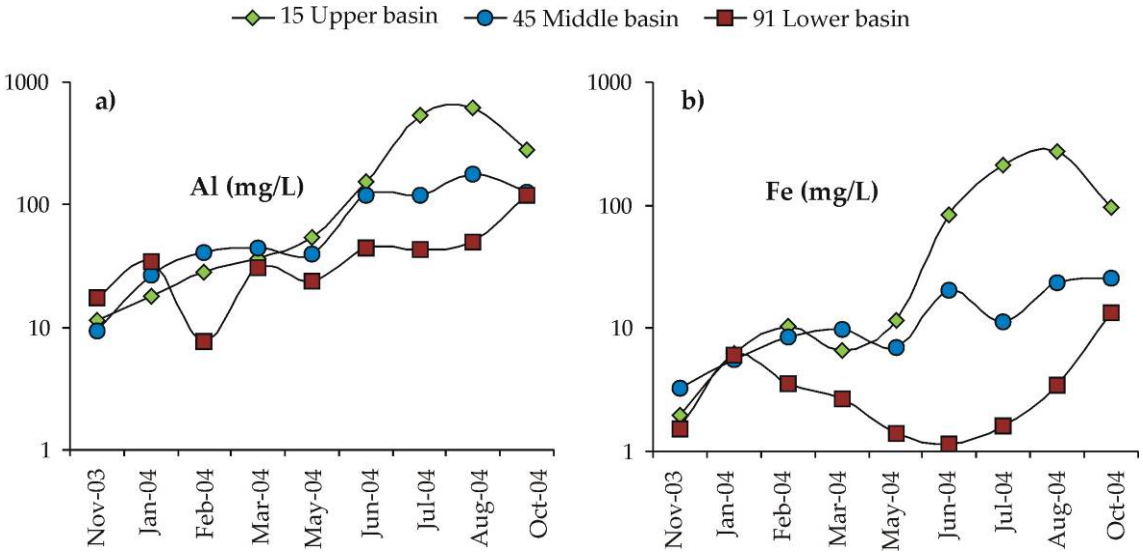
15 Upper basin
45 Middle basin
91 Lower basin
a)
Al (mg/L)
b)
Fe (mg/L)
1000
100
10
1
Nov-03
Jan-04
Feb-04
Mar-04
May-04
Jun-04
Jul-04
Aug-04
Oct-04

Figure 14

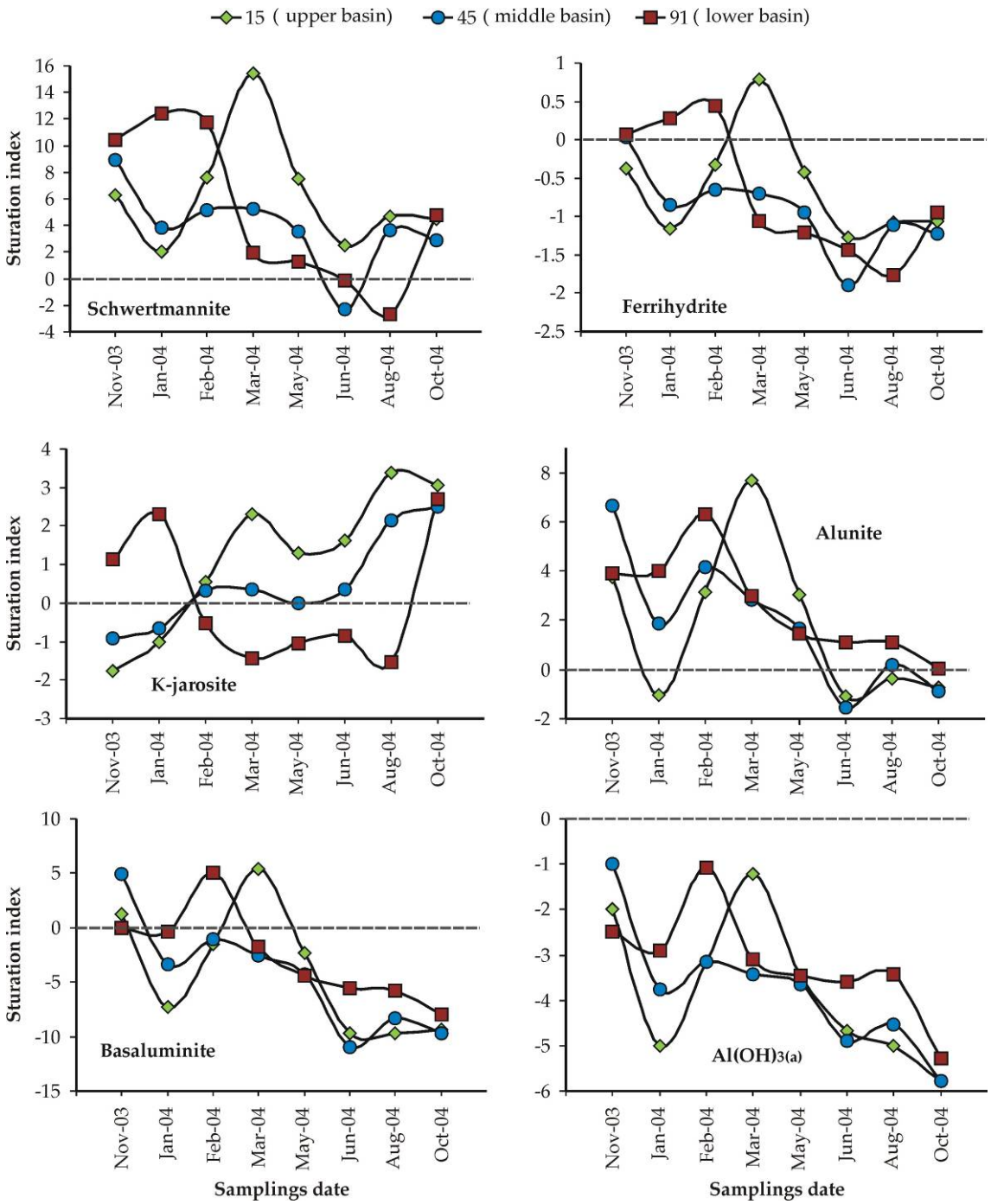
15 (upper basin)
45 (middle basin)
91 (lower basin)
Suturation index
Schwertmannite
Ferrihydrite
K-jarosite
Alunite
Basaluminite
Al(OH)3(a)
Nov-03
Jan-04
Feb-04
Mar-04
May-04
Jun-04
Aug-04
Oct-04
Samplings date

Figure captions

Figure 1. Odiel River Basin location map indicating geology, major mines and sampling points.

Figure 2. Record of (a) daily average rainfall and temperatures in the Odiel River Basin and (b) daily water flow for the Odiel river mouth at Gibraleón during the studied period. The shaded zones display the selected period for the seasonal variation study, and the black points show the date of the samplings.

Figure 3. (a) Piper diagram showing the types of the natural uncontaminated samples. (b) Piper diagram for the uncontaminated samples in two different seasons.

Figure 4. (a) Relationship between sodium and chloride concentration for the uncontaminated samples. (b) Relationship between the concentration of the main components in seawater (Na + Mg + Cl) and the vertical geometric coordinate (Y-UTM).

Figure 5. Evolution of some parameters along the main courses of the Odiel River (a) and Oraque River (b), indicating places of the mines discharging into the river. Distances are kilometres from the headwaters.

Figure 6. Relationships between the redox potential and (a) pH, (b) specific conductance, (c) dissolved oxygen and (d) Fe^{2+}/Fe_t ratio for the contaminated samples.

Figure 7. Relationship between the SO_4^{2-} and iron concentration. Continuous line indicates the theoretical molar ratio Fe/SO_4^{2-} derived from the pyrite oxidation.

Figure 8. Ficklin diagram showing the sum of dissolved base metals (Zn, Cu, Cd, Pb, Co and Ni) for contaminated streams. Black stars represent the downstream evolution of the chemistry of the Meca River.

Figure 9. Relationship between accumulated 30-day rainfall and average values of pH and specific conductance for the contaminated samples.

Figure 10. Principal Component Analysis of results of the hydrological year 2003/04 for two different types of water streams according to the level of pollution. (a) Variables (b) Sampling dates.

Figure 11. Plot of Metal/Fe ratio against pH for contaminated samples.

Figure 12. Temporal behaviour of Fe/sulphate ratio against pH for two different types of samples according to the level of pollution. (see point locations in Fig. 1).

Figure 13. Evolution of Al and Fe concentration along the hydrological year 2003-2004 in three different points of the Odiel river (see Fig. 1 for location).

Figure 14. Evolution of the saturation indexes of some typical minerals in AMD along the hydrological year 2003/2004 in three different points of the Odiel river (see Fig. 1 for location).